

Fermi National Accelerator Laboratory

Fermilab-Conf-92/040-T

Lattice QCD

Andreas S. Kronfeld

Theoretical Physics Group, Fermi National Accelerator Laboratory,
P.O. Box 500, Batavia, IL 60510

February 10, 1992

ABSTRACT

Introductory lectures on lattice field theory with focus on QCD. Presented at the TASI Summer School *Perspectives in the Standard Model*, Boulder, Colorado, June 3-28, 1991.



1 Introduction

One perspective of the Standard Model sees only its enormous success. A good deal of the success is genuine—there are many cases of splendid agreement between experiments and theoretical calculations. But other evidence for the standard model is only circumstantial; agreement is qualitative, but physicists think things will work out, after improvements in the calculations. Other experiments measure the product of a fundamental parameter and a quantity that is calculable in principle, but not (yet) in practice. Consequently, the consistency of the standard model hinges on imprecise or incomplete knowledge. A more modest perspective sees the flaws and worries about the work left to be done.

The situation deteriorates roughly as the reliability of perturbation theory. The obstacles are the technical, and occasionally conceptual, problems of performing non-perturbative calculations. Where do these issues arise?

One place is in the electro-weak symmetry-breaking sector. Results from LEP and the Tevatron imply that the top-quark Yukawa interaction are moderately large. Perturbation theory suggests that the associated running coupling increases at short distances, as does that of the Higgs-boson self-interaction. Hence, non-perturbative methods are needed to ensure that the short-distance behavior is under control. Indeed, lattice field theory has had one of its most significant triumphs in this area, providing a bound on the mass of the Higgs boson, cf. sect. 9.

Non-perturbative phenomena are essential to understanding quantum chromodynamics (QCD), the theory of the strong interactions. The particles observed are mesons and baryons, but the fundamental fields are quarks and gluons. Most properties of the hadrons are inaccessible in perturbation theory. Aside from their mere existence, the most blatant example is the mass spectrum. The lack of an accurate, reasonably precise, calculation of the mass spectrum is a major piece of unfinished business for theoretical particle physics. In addition, a wide variety of other non-perturbative calculations in QCD are necessary to interpret ongoing experiments. For example, it is impossible to extract the Cabibbo-Kobayashi-Maskawa angles without knowing matrix elements of operators in the K , D and B mesons. Furthermore, non-perturbative analyses of quarkonia can determine the strong coupling constant with uncertainties already comparable to perturbative analyses of high-energy data.

These lectures cover lattice field theory, the only general, systematic approach that can address quantitatively the non-perturbative questions raised above. Sects. 2–8 explain how to formulate quantum field theory on a lattice and why lattice field theory is theoretically well-founded. Sect. 9 sketches some analytic calculations in scalar lattice field theory. They serve as an example of how lattice field theory can contribute to particle physics without necessarily using computers. Sect. 10 turns to the most powerful tool in lattice field theory: large-scale Monte Carlo integration of the functional integral. Instead of discussing algorithms in gory detail, the general themes of computational field theory are discussed. The methods needed for spectroscopy, weak matrix elements, and the strong coupling constant are reviewed.

The early successes of lattice gauge theory are not reviewed here. One of the first was the shape of the heavy-quark potential. Lattice gauge theory gives convincing evidence that the potential rises linearly at large distances, which is sufficient for con-

finement. There are many important results on non-Abelian gauge theories at non-zero temperature. For $SU(3)$ there is a first-order transition to a “quark-gluon plasma.” The temperature at which the transition occurs has been determined with precision in the pure gauge theory, and calculations are underway in full QCD (i.e. with quarks). The lectures also do not provide status reports on many of the longstanding problems, such as the light hadron spectrum, where progress has been incremental for several years.

The reason for neglecting these topics is that the intended audience for these lectures are students interested in the interplay between theoretical and experimental physics. Over the next few years more and more results from lattice QCD will become relevant to phenomenology. Non-experts will have to understand what these results mean, how reliable they are, and what can be reasonably expected. Therefore, these lectures give a broad outline of the ideas supporting lattice QCD, why it is a theory, instead of a model. Lattice QCD has already produced reliable calculations that help extract V_{CKM} and α_s —fundamental parameters of the standard model. These calculations are used as examples of how computational methods can yield real results.

2 Field Theory on a Lattice

Without an ultraviolet cutoff, quantum field theory does not make much sense. One way to introduce a cutoff is a lattice. For our purposes it is enough to consider a lattice embedded into d dimensional space-time. A lattice is discrete set of points with connections between nearby neighbors. The connectivity also specifies a hierarchy of elementary cells, from 0-dimensional sites up to d -dimensional polyhedra, which are usually hypercubes, but sometimes simplexes. One-dimensional cells (the connections between neighbors) are called “links,” and two-dimensional cells “plaquettes.” A square lattice ($d = 2$) is depicted in fig. 1. Lattice field theory has field variables only on sites, links, or higher dimensional cells, rather than throughout space-time. Sometimes the lattice is considered to be a discrete approximation to space-time. However, a better perspective is to view space-time as continuous and view the lattice fields as approximate aggregates of continuum fields spread over a region of linear size a .

One way to understand why cutoffs simplify field theory is presented in fig. 2. No one working in the upper left corner has succeeded either in constructing quantum field theories, or in computing quantities that are measured in experiments. Evidently, the mathematics of an uncountably infinite number of degrees of freedom is too daunting. Instead, the most promising avenue of constructive field theory starts in the lower right, and travel to the upper left via the upper right. Analytical calculations of measurable quantities, either in perturbation theory or the expansion sketched in sect. 9, use the lower left corner. The numerical calculations of sect. 10 (as well as analytical calculations concerned with infrared behavior) use the lower right corner.

An obvious question is whether the use of cutoffs affects physical results. For physical reasons one expects that they hardly do. After all, the shortest-distance physics is given by the ultimate theory of particle interactions, and the longest-distance physics by the ultimate theory of cosmology. These fundamental theories ought not be crucial to our understanding of, say, QCD. Similarly, as long as $\Lambda = \pi/a$ and $1/L$ correspond to energy scales different from, say, the QCD energy scale, the cutoffs should only distort physical results only negligibly.

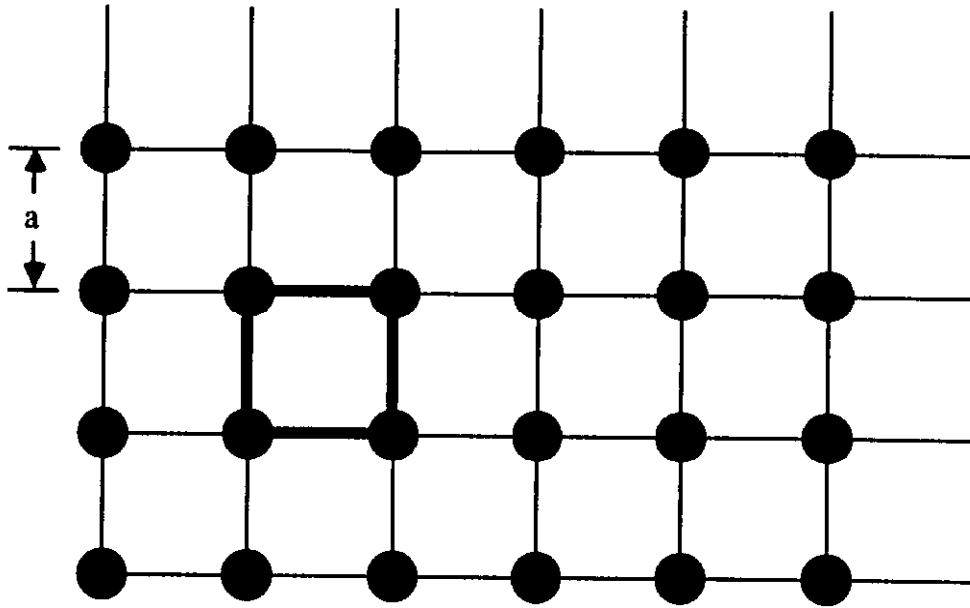


Figure 1: A square two-dimensional lattice. Sites are denoted by dots and links by lines. The bold lines outline a plaquette. The distance separating nearest neighbors is a .

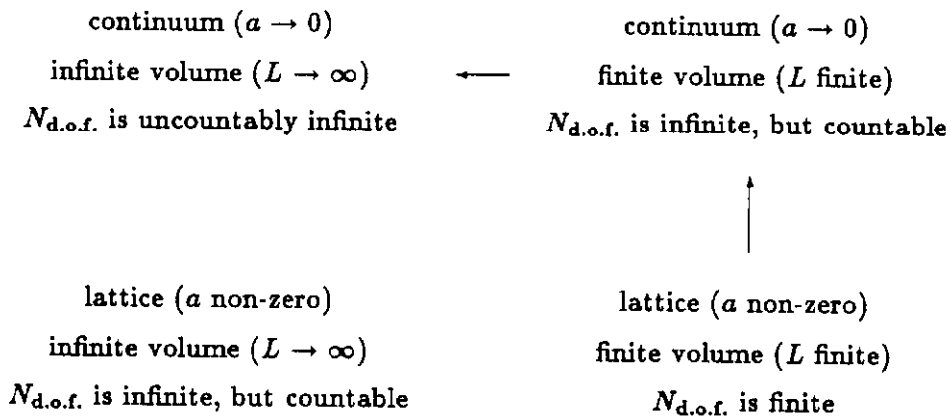


Figure 2: The number of degrees of freedom $N_{d.o.f.}$ in quantum field theories, with and without ultraviolet and infrared cutoffs.

Physically, the lattice cutoff may seem artificial. But if one recalls the standard derivation of the Feynman path integral, one sees a mathematical motivation. Consider quantum mechanics with a Hamiltonian

$$H = \frac{1}{2}\pi^2 + V(\phi) = T + V. \quad (2.1)$$

In anticipation of field theory ϕ denotes the coordinate, and $\pi = -id/d\phi$ denotes the momentum. For reasons that will be explained below, consider the evolution through an imaginary interval $t = -i\tau$, where τ is real. Divide τ into N small intervals and write $a = \tau/N$. Then

$$\langle \phi_N | e^{-iHt} | \phi_0 \rangle = \int \prod_{n=1}^{N-1} d\phi_n \prod_{n=0}^{N-1} \langle \phi_{n+1} | e^{-Ha} | \phi_n \rangle \quad (2.2)$$

gives the amplitude for $|\phi_0\rangle$ to evolve into $|\phi_N\rangle$ during t , expressed as N steps of duration $-ia$. If a is small enough, $e^{-Ha} \approx e^{-T_a} e^{-V_a}$, and it becomes easy to work out the matrix elements:

$$\langle \phi_{n+1} | e^{-Ha} | \phi_n \rangle = \frac{1}{\sqrt{2\pi a}} e^{-aL_n}, \quad (2.3)$$

where

$$L_n = \frac{1}{2} \left(\frac{\phi_{n+1} - \phi_n}{a} \right)^2 + V(\phi_n). \quad (2.4)$$

Identifying $(\phi_{n+1} - \phi_n)/a$ with $-i d\phi/dt$ implies that $-L_n$ is the Lagrangian. Combining eqs. (2.2) and (2.3) gives the path integral

$$\langle \phi_N | e^{-Ht} | \phi_0 \rangle = \lim_{\substack{a \rightarrow 0 \\ N \rightarrow \infty \\ N_a = \tau \text{ fixed}}} \int \prod_{n=1}^{N-1} \frac{d\phi_n}{\sqrt{2\pi a}} \exp \left(-a \sum_{n=0}^{N-1} L_n \right) = \int \mathcal{D}\phi e^{-S}. \quad (2.5)$$

In the last equality the measure $\mathcal{D}\phi = \prod_n d\phi_n / \sqrt{2\pi a}$, the action $S = a \sum_n L_n$, and the $a \rightarrow 0$ limit is implicit.

In field theory both space and time are labels, and the fields represent the degrees of freedom. It is frequently convenient to start with the generating functional of Green's functions. Textbooks give a functional-integral formula

$$Z[j] = \int \mathcal{D}\phi \exp \left(-S + \int d^d x j(x)\phi(x) \right), \quad (2.6)$$

justified by formal manipulations. If one wants to define functional integrals explicitly, eq. (2.5) suggests the following approach: Start with finite intervals L_μ for each space-time direction, and slice them into N_μ tiny intervals of size a . This is a hypercubic lattice. Then

$$Z[j] = \lim_{L_\mu \rightarrow \infty} \lim_{\substack{a \rightarrow 0 \\ N_\mu \rightarrow \infty \\ N_\mu a = L_\mu \text{ fixed}}} \int \prod_n \frac{d\phi_n}{\sqrt{2\pi a}} \exp \left(-a^d \sum_n [\mathcal{L}_n + j_n \phi_n] \right), \quad (2.7)$$

where ϕ_n denotes the field at site n of the lattice, j_n its source, and \mathcal{L}_n is now the Lagrange density associated with site n .

The functional integral over a lattice of finite extent requires boundary conditions on the fields. A natural choice for the time direction would be to project onto the vacuum, or ground state, in the far future and far past. But that would presuppose knowledge of the ground state. Instead, one simply sets the final and initial states equal, and sums over all possibilities. In other words, one uses periodic boundary conditions in time. It is convenient to impose periodic boundary conditions in the spatial directions too.

By analogy with eq. (2.4) the spatial derivatives of the Lagrangian are also replaced by finite differences. For example, consider scalar fields on a d -dimensional hypercubic lattice. The site index n can be taken to be a d -dimensional vector of integers with $x_\mu = an_\mu$. A systematic method to generate a lattice action can be built around operators that translate fields by one lattice spacing in each direction. Define $t_{\pm\mu}$ by

$$t_{\pm\mu}\phi(\mathbf{x}) = \phi(\mathbf{x} \pm a\hat{\mu}), \quad (2.8)$$

acting on the left, and

$$\phi(\mathbf{x}) \overleftarrow{t}_{\pm\mu} = \phi(\mathbf{x} \mp a\hat{\mu}) \quad (2.9)$$

acting on the right. On an infinite lattice or a finite lattice with periodic boundary conditions $\sum_{\mathbf{x}} f(\mathbf{x}) \overleftarrow{t}_{\pm\mu} g(\mathbf{x}) = \sum_{\mathbf{x}} f(\mathbf{x}) t_{\pm\mu} g(\mathbf{x})$, which is the discrete analog on integration by parts. A related property is $t_{\mu}^{\dagger} = t_{-\mu}$.

The action of scalar field theory is

$$S = a^d \sum_{\mathbf{x}} \mathcal{L}_{\mathbf{x}} = a^d \sum_{\mathbf{x}} \left(\frac{1}{2} \partial_{\mu} \phi(\mathbf{x}) \partial_{\mu} \phi(\mathbf{x}) + \frac{1}{2} m_0^2 \phi^2(\mathbf{x}) + V(\phi(\mathbf{x})) \right). \quad (2.10)$$

An obvious discretization sets

$$\partial_{\mu} = \frac{1}{a}(t_{\mu} - 1). \quad (2.11)$$

Then, suppressing the summation sign,

$$\partial_{\mu} \phi(\mathbf{x}) \partial_{\mu} \phi(\mathbf{x}) = \frac{1}{a^2} \phi(\mathbf{x})(t_{-\mu} - 1)(t_{\mu} - 1)\phi(\mathbf{x}) = \frac{1}{a^2} \phi(\mathbf{x})(2 - t_{-\mu} - t_{\mu})\phi(\mathbf{x}). \quad (2.12)$$

In the middle expression the difference operator $(t_{-\mu} - 1)$ can be thought to act either to the right or to the left. After integration by parts, the derivative terms can be written $-\frac{1}{2}\phi(\mathbf{x})\Delta\phi(\mathbf{x})$, where Δ denotes the Laplacian. From eq. (2.12) we see that the most natural lattice Laplacian is

$$\Delta = \frac{1}{a^2}(t_{\mu} + t_{-\mu} - 2). \quad (2.13)$$

Putting eqs. (2.10) and (2.12) together, gives the lattice action.

Exercise 2.1 Re-write the lattice action as

$$S = -a^{d-2} \sum_{\mathbf{x}} \phi(\mathbf{x} + a\hat{\mu})\phi(\mathbf{x}) + a^d \sum_{\mathbf{x}} \left(\left(\frac{1}{2} m_0^2 + da^{-2} \right) \phi^2(\mathbf{x}) + V(\phi(\mathbf{x})) \right). \quad (2.14)$$

For scalar field theory the translation operators are, perhaps, a bit excessive. However, lattice Fermi fields and lattice gauge fields are less trivial, and they can be useful.

To construct a quantum field theory, one must discuss under what circumstances the limits in eq. (2.7) exist. The continuum limit is especially subtle, because it must be taken holding physical quantities (including not only the box size, but also particle

masses, scattering amplitudes, etc.) fixed. This cannot be done without renormalization, as elaborated in sect. 4. Briefly, m_0 and the parameters in $V(\phi)$ must depend on a in a special way, if the limit is to exist.

Usually one ignores mathematical details and treats the limits in eq. (2.7) formally. For perturbation theory and other semi-classical approximations, this approach works fine, because one can check that the results reproduce canonical quantization. Once the correspondence becomes familiar, one can deduce useful information starting from formal functional integrals. However, because the ultraviolet regulator is no longer explicit, one must be aware that some formal arguments are misleading.

In lattice field theory the paradigm is to compute with an explicit ultraviolet cutoff. The advantage is that the generating functional then exhibits an overpowering similarity to the partition function of classical statistical mechanics. Therefore, all the techniques developed in statistical mechanics are available. Some, such as high-temperature expansions exploit a small parameter. However, unlike Feynman perturbation theory, the zeroth-order starting point need not be free field theory. Another widely applied technique is Monte Carlo integration, a numerical evaluation of the functional integral at fixed a and L_μ . Since it does not rely on a small parameter, it offers the most promise for solving QCD. The drawback is that one must work on a sequence of lattices, to reduce and remove the a and L_μ dependence from physical quantities.

3 Some Euclidean Field Theory

Eq. (2.7) is mathematically well-defined, but the time interval through which the fields evolve is imaginary. In perturbation theory, the Wick rotation back to real time can be verified order-by-order. Loop diagrams contain factors

$$d\omega \frac{1}{\omega^2 + E^2}, \quad (3.1)$$

where $E^2 = \mathbf{p}^2 + m^2$. The poles on ω are at $\pm iE$. If one moves them off the imaginary axis $\pm iE \rightarrow \pm iE \pm \frac{1}{2}\varepsilon/E$, one can continue $\omega \rightarrow -i\omega$. The propagator becomes

$$d\omega \frac{i}{\omega^2 - E^2 + i\varepsilon}, \quad (3.2)$$

which is the usual real-time expression, complete with Feynman's $i\varepsilon$ -prescription.

These manipulations are so straightforward in perturbation theory that much work is done with imaginary time. This formalism has been dubbed Euclidean field theory, because most changes are taken care of by using the metric $\text{diag}(1, 1, 1, 1)$. However, at the non-perturbative level the Wick rotation is useless, and one needs another way to relate Euclidean field theory to real-time quantum mechanics. This section explains an approach based on lattice field theory and the transfer matrix [1].

The goals are a Hilbert space of states, a time evolution operator, and a Hamiltonian. We shall use a hypercubic lattice, and, to simplify the formulae, we shall set $a = 1$. Eq. (2.7) treats all d directions on the same footing, but single out the d -th direction to play the role of time. The set of sites \mathbf{x} at fixed time t will be called a timeslice, and $\phi_t = \{\phi(\mathbf{x}, t)\}$ will denote all field variables in timeslice t . Let \mathcal{H} be the Hilbert space

of square-integrable functions over ϕ_t with inner product

$$(\Psi_1, \Psi_2) = \int \mathcal{D}\phi_t \Psi_1^*(\phi_t) \Psi_2(\phi_t), \quad (3.3)$$

where $\mathcal{D}\phi_t = \prod_{\mathbf{x}} d\phi(\mathbf{x}, t)$ is the measure for one timeslice. If the spatial extent of the lattice is finite, \mathcal{H} is precisely the Hilbert space that one would define for this many-degree-of-freedom system. To derive the time-evolution operator, start with the generating functional of eq. (2.7)

$$Z = \int \mathcal{D}\phi e^{-S} \quad (3.4)$$

with a and L_μ fixed, for the time being. (The source is suppressed.) Write the action as

$$S = \sum_t L(\phi_{t+1}; \phi_t), \quad (3.5)$$

where

$$L(\phi_{t+1}; \phi_t) = - \sum_{\mathbf{x}} \phi(\mathbf{x}, t+1) \phi(\mathbf{x}, t) + \frac{1}{2} (U(\phi_{t+1}) + U(\phi_t)). \quad (3.6)$$

Here U denotes all the terms of the Lagrangian that depend on only one timeslice. Next reorganize the integrations in eq. (3.4) as follows

$$Z = \int \prod_t (\mathcal{D}\phi_t \mathcal{K}(\phi_{t+1}, \phi_t)), \quad (3.7)$$

where

$$\mathcal{K}(\phi_{t+1}, \phi_t) = e^{-L(\phi_{t+1}; \phi_t)}. \quad (3.8)$$

The kernel \mathcal{K} defines an operator on \mathcal{H}

$$(\hat{T}\Psi)(\phi_t) = \int \mathcal{D}\phi_u \mathcal{K}(\phi_t, \phi_u) \Psi(\phi_u), \quad (3.9)$$

where \hat{T} is called the transfer operator, or, by abuse of language, the *transfer matrix*. By construction $\mathcal{K}(\phi_u, \phi_t) = \mathcal{K}(\phi_t, \phi_u)$, so for suitably chosen $V(\phi)$ the transfer operator is Hermitian.

The transfer matrix inherits the symmetries of the canonical (lattice) Hamiltonian,

$$H_{\text{can}} = \sum_{\mathbf{x}} \frac{1}{2} \pi^2(\mathbf{x}) + V(\phi(\mathbf{x})). \quad (3.10)$$

Typical examples are internal symmetries and the lattice translations and rotations. Unitary operators generating such symmetries commute with \hat{T} . Consequently, the eigenstates $|\alpha\rangle$ fall into multiplets classified by a maximal set of commuting operators. Furthermore, operators can be decomposed into irreducible representations of the symmetry group, and matrix elements satisfy a Wigner-Eckhart theorem.

The transfer matrix can be used to express the generating functional compactly:

$$Z = \text{Tr}\{\hat{T}^{N_t}\}, \quad (3.11)$$

where N_t is the total number of timeslices in the lattice, and the trace is taken over \mathcal{H} . The eigenvectors $|\alpha\rangle$ and eigenvalues \mathcal{T}_α of the transfer matrix yield an explicit representation:

$$Z = \sum_{\alpha} \langle \alpha | \mathcal{T}_\alpha^{N_t} | \alpha \rangle. \quad (3.12)$$

For future purposes, let us introduce $|0\rangle$ as the state with *largest* eigenvalue \mathcal{T}_0 . This *vacuum* will always be unique, as long as the number of degrees of freedom is finite.

At this stage we have \mathcal{H} , the quantum mechanical Hilbert space, and \mathcal{T} , the evolution operator through imaginary time $t = -ia$. In real time energy eigenstates evolve with $e^{-iE_\beta t}$. This consideration suggests defining the Hamiltonian to be

$$\hat{H} = -\frac{1}{a} \ln \left(\frac{\hat{\mathcal{T}}}{\mathcal{T}_0} \right) = -\frac{1}{a} \sum_{\alpha} |\alpha\rangle \ln \left(\frac{\mathcal{T}_\alpha}{\mathcal{T}_0} \right) \langle \alpha|. \quad (3.13)$$

If it is to be Hermitian, the transfer matrix must not only be Hermitian, but also positive. The Hamiltonian defined in eq. (3.13) is not simply related to the canonical Hamiltonian, eq. (3.10), *unless* the lattice spacing is infinitesimal *and* perturbation theory is reliable. Adapting the language of perturbative quantum field theory, one might say that eq. (3.10) gives the bare Hamiltonian of the cutoff-scale fields, whereas eq. (3.13) gives the renormalized Hamiltonian of the asymptotic states. This relationship and the continuum limit of the transfer matrix is explored in sect. 4.

Exercise 3.1 Consider the partition function of quantum statistical mechanics,

$$Z = \text{Tr}\{e^{-\beta H}\}, \quad (3.14)$$

whereas in eq. (3.11) the trace is in Hilbert space, and β is the inverse temperature. Show that it and the Euclidean field theory generating functional can be expressed by an expression similar to eq. (2.7), but with $\beta = N_t a$ fixed.

For the purposes of these lectures, it is enough to examine positivity of the transfer matrix for free field theories. Let us do so for free scalar field theory, using the action derived in the previous section. In momentum space the translation operators are $t_{\pm\mu} = e^{\pm iap_\mu}$, so it is easy to read off the inverse propagator from eqs. (2.10) and (2.12):

$$\Delta(p) = \sum_{\mu} \frac{2 - e^{-iap_\mu} - e^{iap_\mu}}{a^2} + m_0^2 = \hat{p}^2 + m_0^2, \quad (3.15)$$

where $\hat{p}_\mu = (2/a) \sin(\frac{1}{2}ap_\mu)$. The energy of a particle with momentum \mathbf{p} can be read off from

$$C(t, \mathbf{p}) = \int_{-\pi/a}^{\pi/a} \frac{d\omega}{2\pi} \frac{e^{i\omega t}}{\omega^2 + \hat{\mathbf{p}}^2 + m_0^2}. \quad (3.16)$$

The ω integral can be performed by contour integration, using the variable $z = e^{i\omega \text{sgn}(t)}$. One finds

$$C(t, \mathbf{p}) = \frac{a}{2 \text{sh}(Ea)} e^{-E|t|} \quad (3.17)$$

where

$$4 \text{sh}^2(\frac{1}{2}Ea) = a^2(m_0^2 + \hat{\mathbf{p}}^2). \quad (3.18)$$

At non-zero a the energy, as defined by the transfer matrix, is E and not $\sqrt{m_0^2 + \mathbf{p}^2}$.

Exercise 3.2 Verify eq. (3.17). Verify also that the continuum propagator and dispersion relation are recovered for $ap, am_0 \ll 1$.

In verifying eq. (3.17), one notices that the combination $T(\mathbf{p}) = e^{-Ea}$ arises. These $T(\mathbf{p})$ are the single-particle eigenvalues of the transfer matrix, positive as desired.

Exercise 3.3 Suppose the kinetic part of the action had been discretized using $(t_\mu - t_{-\mu})^2/(4a^2)$ instead of $(t_\mu + t_{-\mu} - 2)/a^2$ for the lattice Laplacian. Show that the single-particle eigenvalues of the transfer matrix are $T_\pm(\mathbf{p}) = \pm e^{-Ea}$, and find the expression for E . Note that some of the eigenvalues are negative, but \hat{T}^2 is positive.

Sometimes, as in Exercise 3.3, a one-timeslice transfer matrix has negative eigenvalues, but an l -timeslice transfer matrix is positive. As long as l is small, it is then possible to define an acceptable Hamiltonian via

$$H = -\frac{1}{la} \ln \left(\frac{\hat{T}^l}{T_0^l} \right), \quad (3.19)$$

where T^l is the l -timeslice transfer matrix.

To understand the transfer-matrix formalism further, consider the correlator of two functions defined on a single timeslice.

$$\langle \mathcal{O}_1(\phi_t) \mathcal{O}_2(\phi_0) \rangle = \frac{1}{Z} \int \mathcal{D}\phi \mathcal{O}_1(\phi_t) \mathcal{O}_2(\phi_0) e^{-S(\phi)}. \quad (3.20)$$

By time-translation invariance \mathcal{O}_2 is at placed at time 0. Reorganizing the integrations as above

$$\langle \mathcal{O}_1(\phi_t) \mathcal{O}_2(\phi_0) \rangle = \quad (3.21)$$

$$\frac{1}{Z} \int \prod_t \mathcal{D}\phi_t \mathcal{K}(\phi_0, \phi_{N_t-1}) \cdots \mathcal{K}(\phi_{t+1}, \phi_t) \mathcal{O}_1(\phi_t) \mathcal{K}(\phi_t, \phi_{t-1}) \cdots \mathcal{K}(\phi_1, \phi_0) \mathcal{O}_2(\phi_0).$$

In operator form

$$\langle \mathcal{O}_1(\phi_t) \mathcal{O}_2(\phi_0) \rangle = \frac{\text{Tr}[\hat{T}^{N_t-t} \hat{\mathcal{O}}_1 \hat{T}^t \hat{\mathcal{O}}_2]}{\text{Tr}[\hat{T}^{N_t}]}, \quad (3.22)$$

where $\hat{\mathcal{O}}_i|\phi\rangle = \mathcal{O}_i(\phi)|\phi\rangle$. Introduce complete sets of eigenstates of T into eq. (3.22), yielding

$$\langle \mathcal{O}_1(\phi_t) \mathcal{O}_2(\phi_0) \rangle = \frac{1}{Z} \sum_{\alpha, \beta} T_\alpha^{N_t-t} \langle \alpha | \hat{\mathcal{O}}_1 | \beta \rangle T_\beta^t \langle \beta | \hat{\mathcal{O}}_2 | \alpha \rangle. \quad (3.23)$$

If $N_t \gg t$, then the largest eigenvalue dominates the α sums in eqs. (3.12) and (3.23). Combining these equations in this limit, gives the equation of greatest practical value in lattice QCD:

$$\langle \mathcal{O}_1(\phi_t) \mathcal{O}_2(\phi_0) \rangle = \sum_\beta \langle 0 | \hat{\mathcal{O}}_1 | \beta \rangle \langle \beta | \hat{\mathcal{O}}_2 | 0 \rangle e^{-tE_\beta}, \quad (3.24)$$

where $E_\beta = -\ln(T_\beta/T_0)$.

Exercise 3.4 Consider eq. (3.22) when $N_t \gg N_t - t$, and derive the finite N_t corrections to eq. (3.24).

Exercise 3.5 Extend the analysis to higher-point correlation functions

$$\langle \mathcal{O}_1(\phi_{t_1}) \mathcal{O}_2(\phi_{t_2}) \dots \mathcal{O}_k(\phi_{t_k}) \rangle. \quad (3.25)$$

Pay attention to time order!

The great value of eq. (3.24), and its generalization for higher-point functions, Exercise 3.5, is that it reveals precisely which particle properties are accessible from Euclidean field theory. First, by appropriately choosing operators \mathcal{O}_i and studying the exponential fall-off of eq. (3.24), one can determine the energy spectrum. For single stable particles at rest these energies are the masses. From the energies of scattering state and resonance it is possible (though not especially straightforward) to extract more detailed dynamical information such as scattering lengths and widths. Second, the matrix elements of local operators can be extracted from analyzing two- and higher-point correlators.

Secs. 5 and 6 discuss lattice actions for fermions and gauge fields. The transfer matrix formalism applies in those case, but with more technicalities, so the reader is referred to the literature [2, 3].

4 Non-Perturbative Renormalization

This section discusses how to take the continuum limit prescribed in eq. (2.7). The continuum limit is the same as the removal of the ultraviolet cutoff, identifying $\Lambda = \pi/a$. From perturbative treatments one knows that renormalization is essential: this section outlines the non-perturbative version [1].

In the previous sections, the lattice spacing a appears explicitly, and it may seem obvious how to take the $a \rightarrow 0$ limit. However, one can only compute dimensionless quantities such as aE_α . Physical units for E_α and the box sizes L_μ (cf. eq. (2.7)) are best specified through a fiducial energy E_1 . Holding E_α/E_1 , $E_1 L_\mu$, and other physical quantities fixed while $aE_1 \rightarrow 0$ can be called the *quantum* continuum limit. By contrast, the $a \rightarrow 0$ limit of the action, rather than the generating functional, can be called the *classical* continuum limit.

The previous sections tacitly neglected interactions. With interactions the physical (or renormalized) mass is related to the bare mass by $m_R^2 = m_0^2 + ca^{-2}$, neglecting logarithms, where c depends on the ultraviolet regulator. In the quantum continuum limit, m_R is held fixed, rather than m_0 , as $a \rightarrow 0$. Clearly this is possible only if m_0 depends on a in a suitable way. More generally, an action

$$S = \sum_n K_n(a) S_n, \quad (4.1)$$

where S_n denotes various local monomials of the fields, can possess a quantum continuum limit only if the couplings K_n are functions of the lattice spacing. We shall use \mathcal{S} to denote the space of actions or, equivalently, the space of couplings. One should keep in mind that the K_n are “bare” quantities in the action.

To discover the location in \mathcal{S} of the quantum continuum limit, one expects certain features in the spectrum of the transfer matrix. The Hilbert space must exhibit a subspace \mathcal{H}_p with eigenvalues $T_\alpha = T_0 e^{-aE_\alpha}$ such that $aE_\alpha \ll 1$. ($E_0 = 0$, by definition.) We have already mentioned that ratios of energies $aE_\alpha/aE_1 = E_\alpha/E_1$ must remain

constant. Flavor and chiral symmetries of fermions, broken in lattice formulations, must be restored. For L_μ large enough, \mathcal{H}_p must exhibit multiplets respecting rotational invariance, as well as mass shells obeying $E_\alpha^2 = m_\alpha^2 + p_\alpha^2$. In short, the states comprising \mathcal{H}_p must comply with all requirements of the physical part of the Hilbert space.

For generic points in \mathcal{S} there is no reason this physical Hilbert space should emerge. One would like to know if it is possible at all and, if so, develop tools to identify where. Let us re-write eq. (2.7) as

$$Z = \lim_{L_\mu \rightarrow \infty} \lim_{\substack{a \rightarrow 0 \\ N_\mu \rightarrow \infty \\ N_\mu a = L_\mu \text{ fixed}}} Z(N_\mu; K_n(a)), \quad (4.2)$$

and consider an associated partition function

$$Z(K_n) = \lim_{N_\mu \rightarrow \infty} Z(N_\mu; K_n) \quad (4.3)$$

of classical statistical mechanics. The particle-physics couplings K_n correspond to J_n/ϑ , where J_n is some parameter, for example a chemical potential, and ϑ is the temperature. Suppose $Z(K_n)$ exhibits a second-order phase transition¹ somewhere in \mathcal{S} . From the theory of critical phenomena one knows that the transfer matrix has eigenvalues of the form $T_0 e^{-1/\xi}$ with $\xi \rightarrow \infty$ as the transition is approached. Identifying $\xi = 1/aE_1$, one concludes that the most essential requirement of the quantum continuum limit arises at a second-order phase transition. Indeed, to re-state the point more strongly, only after second-order phase transitions have been identified for $Z(K_n)$ can the $a \rightarrow 0$ limit in eq. (4.2) be defined.

It is perhaps worthwhile digressing to distinguish the phase structure of the lattice model of eq. (4.3) from thermodynamics of the elementary particles, described by the quantum field theory. The formalism of sects. 2 and 3 leans on the Schrödinger formulation of field theory; the field's degrees of freedom live in $d - 1$ space dimensions and propagate forward in (imaginary) time. The associated thermodynamics would be studied through quantum statistical mechanics of this $(d - 1)$ -dimensional system. If the temperature—the real-world temperature, not ϑ —is only thermodynamic variable, one can use the formalism of Exercise 3.1. Phase transitions do arise in the Standard Model and have implications for astrophysics and cosmology. But, this is *not* the phase-transition structure sought here. The sought-after phase transition must appear in the d -dimensional system whose partition function is defined in eq. (4.3).

Let us return to the discussion of the quantum continuum limit. A region $\mathcal{S}_c \subset \mathcal{S}$ of second-order phase transitions must be identified. As a rule, $\dim \mathcal{S}_c < \dim \mathcal{S}$. Because critical behavior of $Z(K_n)$ appears on \mathcal{S}_c , it is called the critical surface. Finding its location is not as daunting as one might fear. Sometimes the critical surface extends to or coincides with (part of) the boundary of \mathcal{S} , i.e. to extreme values of one or more of the couplings. Then an expansion in a small parameter often yields either the location of the critical surface or, even better, a quantitative description of it. In other cases, \mathcal{S}_c separates phases of broken vs. unbroken symmetry. Then there is generally a diagnostic

¹The “thermodynamic” limit $N_\mu \rightarrow \infty$ appears in eq. (4.3) to make the location and order of phase transitions unambiguous.

quantity, called the order parameter, whose average value changes rapidly at the phase transition.

Once the critical surface has been identified, one can set up the quantum continuum limit. It is taken along a trajectory in \mathcal{S} , as implied by the notation $K_n(a)$ in eq. (4.2). The trajectory ends on \mathcal{S}_c . Before prescribing it off the critical surface, one needs some understanding of the dynamics of the partition function $Z(K_n)$. A flexible approach is the renormalization group. In this context a renormalization group is any set of transformations generating an ultraviolet-regulated effective action from a microscopic action, valid at shorter distances. (The microscopic action may, in turn, be an effective action too.) The choice of renormalization-group transformation is analogous to the choice of a scheme in perturbative renormalization. In the end, the physics should not depend on the choice, which one makes according to calculational convenience.

Let the renormalization group relate an action with ultraviolet cutoff $a \neq 0$ to one with cutoff λa . Calculations of eigenvalues of the transfer matrix, or other convenient observable quantities, yield a relation between the couplings,

$$K_m(\lambda a) = \Psi_m^{(\lambda)}(K_n(a)), \quad (4.4)$$

or, in differential form,

$$\frac{dK_m}{dt} = \psi_m(K_n), \quad (4.5)$$

where $\lambda = e^t$. These renormalization-group equations map out trajectories in \mathcal{S} . It is useful to think of a particle with coordinates K_n and an equation of motion given by eq. (4.5). If one can write² $\psi_m = -\partial\mathcal{F}/\partial K_m$, at least after appropriate change of variables, it is easy to envision how the particle moves. As t increases it slides to decrease \mathcal{F} , spending long intervals of t near points with $\psi_m(K_n) \approx 0$. Points K_n^* with $\psi_m(K_n^*) = 0$ are called fixed points, because if the particle flows into one, it never flows out. At a fixed point the couplings do not change. From eq. (4.4) $K_m^*(\lambda a) = K_m^*(a)$; hence, $\lambda a = a$. At a fixed point either $a = 0$ or $a = \infty$. The quantum continuum limit is defined at the critical ($a = 0$) fixed points. The $a = \infty$ ones will be considered later.

A critical fixed point is a saddle point: some directions leading out of the fixed point increase \mathcal{F} , some decrease \mathcal{F} , and others may be flat. An example with one stable and one unstable direction is sketched in fig. 3, using the Rocky Mountains as a model. To quantitatively analyze the fixed point one can linearize eq. (4.5) about the fixed point [4]:

$$\frac{dK_m}{dt} = \mathcal{M}_{mn}(K_n - K_n^*), \quad (4.6)$$

up to terms of order $(K_n - K_n^*)^2$, where

$$\mathcal{M}_{mn} = \left. \frac{\partial \psi_m}{\partial K_n} \right|_{K_n^*}. \quad (4.7)$$

Diagonalizing $\mathcal{M} = V^{-1}DV$, defining $h_n = \sum_m V_{nm}(K_m - K_m^*)$, and manipulating eq. (4.6), $dh_n/dt = D_n h_n$ or

$$h_n = h_{n,0} e^{D_n t} = h_{n,0} \left(\frac{a_t}{a_0} \right)^{D_n}, \quad (4.8)$$

²This assumption is restrictive, but it gives an intuitive feel for solutions to the renormalization-group equations.

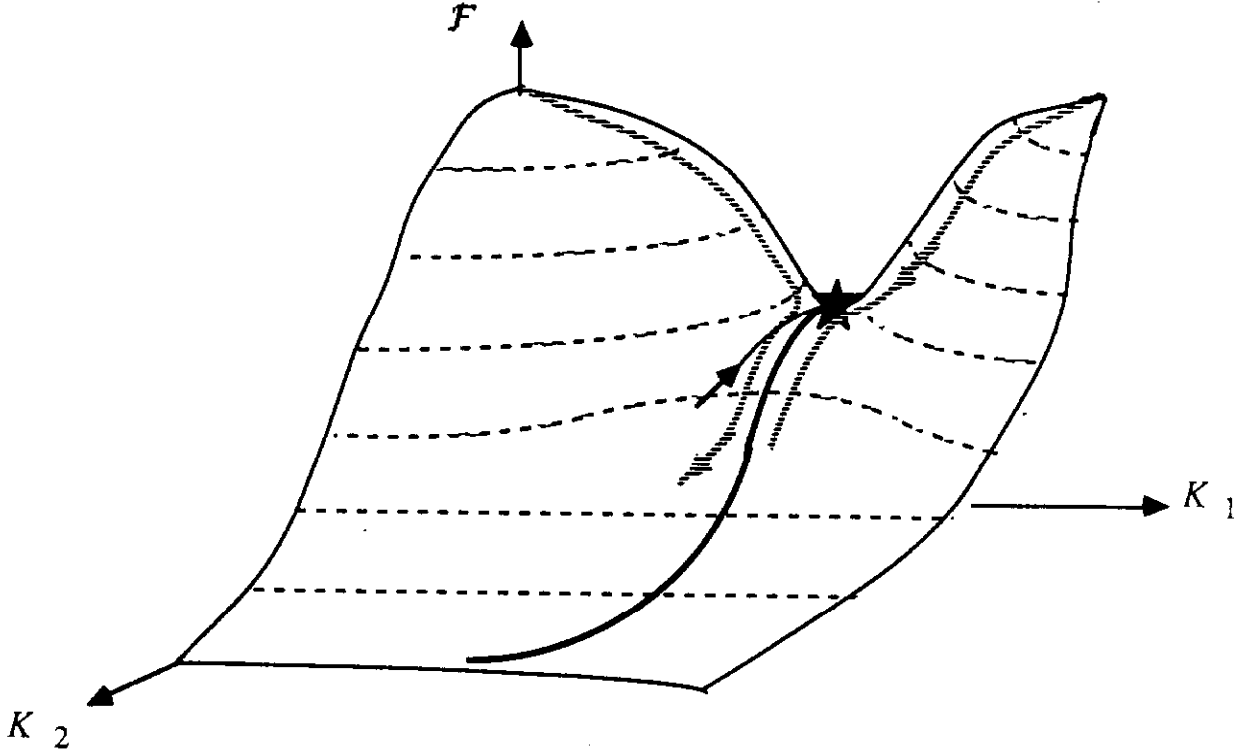


Figure 3: Alpine illustration of renormalization group flows on Mount $\mathcal{F}(K)$. The dotted lines are at constant \mathcal{F} . The plane $K_2 = 0$ is the critical surface. The star denotes the critical fixed point. The skier's tracks pointing downhill are renormalization group trajectories. The solid line pointing uphill gives a trajectory for taking the quantum continuum limit. The bold line is the renormalized trajectory.

where a_0 and $h_{n,0}$ are the initial cutoff and coupling, and $a_t = e^t a_0$. Eq. (4.8) shows that D_n is the scaling dimension of coupling h_n . Because of their role in effective actions with increasing t , if $D_n > 0$ the coupling is called relevant, if $D_n < 0$ it is called irrelevant, and if $D_n = 0$ it is called marginal. For marginal operators, one can expand eq. (4.5) to higher order in $K_n - K_n^*$. If quadratic order suffices, one has $dh_n/dt = b_n h_n^2$ or

$$h_n = \frac{h_{n,0}}{1 - h_{n,0} b_n t} = \frac{h_{n,0}}{1 - h_{n,0} b_n \ln(a_t/a_0)}. \quad (4.9)$$

If $h_{n,0} b_n > 0$ the coupling is marginally relevant, and if $h_{n,0} b_n < 0$ it is marginally irrelevant. Eqs. (4.8) and (4.9) can be re-written in terms of dimensionful renormalization-group invariants

$$\mu_n = \begin{cases} a^{-1} e^{-1/b_n h_n} & \text{for marginal couplings} \\ a^{-1} h_n^{1/D_n} & \text{otherwise,} \end{cases} \quad (4.10)$$

modified by higher-order corrections to eq. (4.6). As usual a is defined through the fiducial energy E_1 .

This description of the fixed point allows us to construct the quantum continuum limit. The relevant couplings shall flow into the fixed point as dictated by the renormalization-group equations, now with $t < 0$. On the other hand, the irrelevant couplings must be forced to vanish. The uphill line in fig. 3 shows a possibility when there is one irrelevant and one relevant coupling (K_1 and K_2 in fig. 3, respectively). As long as an irrelevant parameter is small, perturbation theory in h_n suggests that physical quantities will be contaminated by cutoff artifacts of order $h_n a^{|\mathcal{D}_n|}$. Except for these small effects, the physics depends only on the parameters μ_n for the relevant (and marginally relevant) couplings. These correspond to the N_r unstable directions at the fixed point. If the fixed point is to have much predictive power, N_r should be small, especially since the dimension of \mathcal{S} is not really bounded. In perturbative quantum field theory, the requirement of a small number of parameters boils down to the criterion of renormalizability. The terminology used is a bit different: relevant, marginal, and irrelevant couplings correspond to super-renormalizable, renormalizable, and non-renormalizable, respectively; marginally relevant corresponds to asymptotically free. This correspondence demonstrates that the couplings have been treated the same way in both paradigms.³

Consider now the surface \mathcal{S}_R where all irrelevant couplings vanish. In fig. 3 this is the bold line. Trajectories in \mathcal{S}_R connect the saddle point to a minimum of \mathcal{F} . A minimum, incidentally, is a fixed point with $a = \infty$. Actions on \mathcal{S}_R have $a \neq 0$, but they describe the same physics as the fixed point! In other words, they represent fully renormalized actions. The trajectories in \mathcal{S}_R are, therefore, called renormalized trajectories. In particular, for a fixed point with only one relevant parameter, there is a single renormalized trajectory. The renormalized trajectories provide an alternative definition of the quantum continuum limit. Unless one has an exact solution of eq. (4.3), however, one can only pin down \mathcal{S}_R approximately. For example, an analytical expansion yields the renormalized trajectory to the order computed. A numerical Monte Carlo calculation with an explicit choice of K_n , on the other hand, misses \mathcal{S}_R by $O(a^n)$, unless a miracle occurs. Nevertheless, renormalized trajectories only offer an opportunity to improve the approach to the continuum limit, to reduce the magnitude of the cutoff artifacts, cf. sect. 8.

It is probably useful to illustrate these abstract ideas with two examples closely related to the standard model. In both examples the renormalization group equations are taken from perturbation theory. Hence, it is not necessary to use a lattice for the ultraviolet cutoff; Pauli-Villars or dimensional regulators will do.

The first example is pure gauge theory for $d = 4$. Since the lattice action for gauge fields is introduced in sect. 6 we shall use a momentum space cutoff Λ ($\cong \pi/a$). The action is $S = (1/4g_0^2) \int d^4x (F_{\mu\nu}^a)^2$, where g_0^2 corresponds to K in the general discussion. As a bare coupling, g_0^2 is a function of Λ . According to the procedure outlined above, one must compute, say, the four gluon scattering amplitude as a function of $g_0^2(\Lambda)$ and Λ and demand that the implicit and explicit Λ -dependence cancel. To one loop one obtains

³The reader may have noticed that marginally irrelevant couplings are treated differently. The last paragraph of this section clarifies the difference.

the renormalization-group equation

$$\frac{dg_0^2}{dt} \approx bg_0^4, \quad (4.11)$$

where $b > 0$ and $d/dt = -\Lambda d/d\Lambda$. The logic is similar, but not identical to, the derivation of the Callan-Symanzik equation. Not surprisingly, b is (minus) the first Callan-Symanzik coefficient. Eq. (4.11) shows that $g_0^2 = 0$ is a fixed point, and the gauge coupling is marginally relevant. Hence, the renormalized theory is determined by one dimensionful scale. To one loop it is $a^{-1} \exp(1/bg_0^2)$. In QCD this parameter is, up to a scheme-dependent factor, Λ_{QCD} . These days, the $\overline{\text{MS}}$ scheme is the most popular, because it is so convenient in perturbation theory. In the long run, a better convention would use a scale defined by a physics that is accessible to non-perturbative and perturbative calculations, as well as experiments.

The second example is scalar field theory with $V(\phi) = (g_0/4!)\phi^4$. This action has a field-inversion symmetry $\phi \mapsto -\phi$. There are now two coupling constants, in the sense of eq. (4.1), $h_m = a^2 m_0^2$ and $h_g = a^{4-d} g_0 > 0$. In perturbation theory the renormalization-group equations are

$$\begin{aligned} \frac{dh_m}{dt} &= 2h_m + ch_g, \\ \frac{dh_g}{dt} &= (4-d)h_g + bh_g^2, \end{aligned} \quad (4.12)$$

where c depends on the regulator (e.g. lattice vs. Pauli-Villars), but $b < 0$ does not. The perturbative fixed point⁴ is $h_m = h_g = 0$. Near the fixed point the field-inversion symmetry is unbroken for $m_0^2 > 0$ and spontaneously broken for $m_0^2 < 0$. The perturbative fixed point is not enlightening for $d \neq 4$: The mass coupling h_m is relevant for all d , but the self-coupling h_g is irrelevant (relevant) for $d > 4$ ($d < 4$). However, for $d = 4$ the self-coupling h_g is marginally irrelevant. If the continuum limit of the ϕ^4 theory is defined at the perturbative fixed point, g_0 must vanish. This is the so-called ‘‘triviality’’ of the ϕ^4 theory: if g_0 vanishes, so does the physical four-scalar coupling. The same results hold for multi-component scalar field theories, such as the Higgs sector of the standard model. The way out is to find another fixed point. A futile (so far) search for a non-trivial fixed point has been carried out by many notable authors. A more pragmatic view, which will be taken up again in sect. 9, is to keep Λ finite and view the cutoff ϕ^4 action as an effective action. This is certainly the correct view for anyone who believes that there is a more fundamental explanation of electroweak symmetry breaking than the scalar fields of the standard model.

5 Lattice Fermi Fields

For scalar field theories the most straightforward discretization of the derivatives led to a lattice field theory with positive transfer matrix. Consider now the (free) Dirac action

$$S_{\text{F}} = -a^4 \sum_x \bar{\psi}(x)(\not{\partial} + \not{m}_0)\psi(x), \quad (5.1)$$

⁴This fixed point is often called Gaussian, because at $h_g = 0$ the functional integral is Gaussian.

where $\partial = \gamma_\mu \partial_\mu$ and $\{\gamma_\mu, \gamma_\nu\} = 2\delta_{\mu\nu}$ in Euclidean field theory.⁵ On the lattice one wants ∂_μ to be a difference operator. The simple choices $t_\mu - 1$ and $1 - t_{-\mu}$ are not anti-Hermitian, so particles and anti-particles would propagate differently. Therefore, they are not acceptable. However, the symmetric difference operator $\frac{1}{2}(t_\mu - t_{-\mu})$ is anti-Hermitian, so it is an obvious first candidate.

As in sect. 2, let us check the positivity of the free action with $\partial_\mu = (t_\mu - t_{-\mu})/(2a)$; the action obtained with this naive discretization will be denoted S_{NF} . The inverse propagator is $i\mathcal{J}(p) + m_0$, where $S_\mu(p) = \sin(ap_\mu)/a$. Fourier transforming in p_0 yields

$$C(t) = \frac{a}{\text{sh}(2Ea)} \left[e^{-Et} \left(a^{-1} \text{sh}(Ea) \gamma_0 - i\mathbf{S} \cdot \boldsymbol{\gamma} + m_0 \right) \right. \\ \left. - \left(-e^{-Ea} \right)^{t/a} \left(a^{-1} \text{sh}(Ea) \gamma_0 - i\mathbf{S} \cdot \boldsymbol{\gamma} - m_0 \right) \right] \quad (5.2)$$

for $t > 0$, and a similar expression for $t < 0$. As always, E denotes the transfer-matrix definition of the energy. It obeys a dispersion relation

$$\text{sh}^2(Ea) = a^2(\mathbf{S}^2 + m_0^2) \quad (5.3)$$

that reduces the relativistic one, when $pa, m_0a \ll 1$.

There are many problems with these naive lattice fermions, which one can read off eq. (5.2). First, concentrate on the first parentheses. For $\mathbf{p} = 0$ it is proportional to $(1 + \gamma_0)$, as expected. But, from eq. (5.3) and the definition of $S_\mu(p)$, any state with momentum $p_i = \pi/a - q_i$ has the same energy as a state with $p_i = q_i$. Next, concentrate on the second parentheses in eq. (5.2). For $\mathbf{p} = 0$ it is proportional to $(1 - \gamma_0)$, contrary to expectations. Furthermore, its eigenvalue of the (single-timeslice) transfer matrix is $-e^{-Ea} < 0$, so the Hamiltonian must be defined by $\hat{H} = -\ln(\hat{T}^2/\mathcal{T}_0^2)/(2a)$, as in eq. (3.19). All in all, with the naive lattice action one Fermi field produces 2^d fermions.

These bad features are the first signature of a pervasive problem, the ‘‘fermion doubling problem.’’

To get rid of the second parentheses in eq. (5.2), Wilson took a hint from the $\mathbf{p} = 0$ states. Wilson fermions [5] replace $-\gamma_0(t_0 - t_{-0})/2$ with $\frac{1}{2}(1 - \gamma_0)(t_0 - 1) + \frac{1}{2}(1 + \gamma_0)(t_{-0} - 1)$. Then only particles propagate ‘‘forward in time,’’ and only anti-particles propagate ‘‘backward in time.’’ (The field operator ψ annihilates particles and creates anti-particles.) Using this prescription in the spatial directions should, by symmetry, eliminate the other unwanted states. The derivative operator is thus

$$\frac{1}{2a}(1 - \gamma_\mu)(t_\mu - 1) + \frac{1}{2a}(1 + \gamma_\mu)(t_{-\mu} - 1) = -\partial + \frac{a}{2}\Delta, \quad (5.4)$$

where, as before, $\partial_\mu = (t_\mu - t_{-\mu})/(2a)$ and $\Delta = (t_\mu + t_{-\mu} - 2)/a^2$. In other words the Wilson fermion action

$$S_{\text{WF}} = S_{\text{NF}} + \frac{a}{2} \sum_{\mathbf{x}} \bar{\psi}(\mathbf{x}) \Delta \psi(\mathbf{x}) \quad (5.5)$$

is obtained by adding to the naive action a term, called the Wilson term, that is irrelevant by power counting. Frequently one defines the hopping parameter K by $(2K)^{-1} = m_0a + d$ and writes

$$S_{\text{WF}} = K \sum_{\mathbf{x}, \mu} \bar{\psi}(\mathbf{x}) [(1 - \gamma_\mu)t_\mu + (1 + \gamma_\mu)t_{-\mu}] \psi(\mathbf{x}) - \sum_{\mathbf{x}} \bar{\psi}(\mathbf{x}) \psi(\mathbf{x}). \quad (5.6)$$

⁵ Euclidean γ matrices are Hermitian, $\gamma_\mu^\dagger = \gamma_\mu$, and $\gamma_\mu^2 = 1$.

Eq. (5.6) assumes a different normalization of the Fermi fields, which is of no consequence, because it is unobservable.

The inverse propagator is now $K(2ia\mathcal{S}(p) + a^2\hat{p}^2 - 2d) + 1$. Again, let us check positivity. The time dependence of the propagator is

$$C(t) = \frac{ae^{-Et} \operatorname{sh}(Ea)\gamma_0 - ia\mathbf{S} \cdot \boldsymbol{\gamma} + am_0 + \frac{1}{2}a^2\hat{p}^2 - 2\operatorname{sh}^2(\frac{1}{2}Ea)}{2\operatorname{sh}(Ea) [1 - K[2(d-1) + a^2\hat{p}^2]]} \quad (5.7)$$

for $t > 0$. The peculiar denominator of eq. (5.7) appears because the ψ does not have the conventional normalization. The energy depends on $m_0 = (1 - 2dK)/(2Ka)$ and p through

$$\operatorname{ch}(Ea) = 1 + \frac{1}{2} \frac{(m_0a + \frac{1}{2}a^2\hat{p}^2)^2 + S^2}{1 + m_0a + \frac{1}{2}a^2\hat{p}^2}. \quad (5.8)$$

Wilson fermions achieve the objective of removing all unwanted states. Neither the $T < 0$ states appear, nor are there low-lying states with $p_i \sim \pi/a$.

Exercise 5.1 Verify that eq. (5.7) is proportional to $1 + \gamma_0$ for $p = 0$. In a similar vein, derive $C(t)$ for $t < 0$ and verify that it is proportional to $1 - \gamma_0$ for $p = 0$.

There is, however, a drawback. Under chiral transformations

$$\psi(\mathbf{x}) \mapsto e^{i\alpha\gamma_5} \psi(\mathbf{x}), \quad \bar{\psi}(\mathbf{x}) \mapsto \bar{\psi}(\mathbf{x})e^{i\alpha\gamma_5}, \quad (5.9)$$

the Wilson term is not invariant,

$$\frac{a}{2} \sum_{\mathbf{x}} \bar{\psi}(\mathbf{x}) \Delta \psi(\mathbf{x}) \mapsto \frac{a}{2} \sum_{\mathbf{x}} \bar{\psi}(\mathbf{x}) \Delta e^{i2\alpha\gamma_5} \psi(\mathbf{x}). \quad (5.10)$$

The light pseudo-scalar meson spectrum suggest that QCD has approximate chiral symmetries. Because the pseudo-scalars are “almost massless” the symmetry must be realized in the Goldstone mode, but since they are not massless, there must be a small explicit breaking. In the Wilson formulation two terms break the chiral symmetry explicitly. In the notation of eq. (5.5), they are the local term proportional to m_0 and the Wilson term. Hence, to describe QCD on the lattice, m_0 must be tuned carefully to counter-act most, but not all, of the breaking from the Wilson term.

An obvious question is whether it is possible to find a fermion action that retains chiral symmetries, as well as other desirable properties. The answer is no. The Nielsen-Ninomiya theorem [6] states that there is no local fermion action that has full chiral symmetry, no additional states, and a real, positive transfer matrix. This result has many important implications. The most significant is that chiral lattice gauge theories are difficult to formulate. (At present, the most promising approaches evade the Nielsen-Ninomiya theorem by adding additional fields. Since no proposal has been proven workable, chiral gauge theories will not be considered further in these lectures.)

Another popular lattice formulation [7] of fermions starts with S_{NF} and makes a unitary transformation (for $d = 4$),

$$\psi(\mathbf{x}) = T(\mathbf{x})\chi(\mathbf{x}), \quad \bar{\psi}(\mathbf{x}) = \bar{\chi}(\mathbf{x})T^\dagger(\mathbf{x}) \quad (5.11)$$

where [8]

$$T(\mathbf{x}) = \gamma_1^{n_1} \gamma_2^{n_2} \gamma_3^{n_3} \gamma_4^{n_4}. \quad (5.12)$$

As usual n_μ denotes a vector of integers, $x_\mu = an_\mu$, so this transformation is valid only on the lattice. Substituting eq. (5.11) into eq. (5.1) yields

$$S_{SF} = -a^4 \sum_{x,\alpha} \bar{\chi}_\alpha(x) (\eta_\mu(x) \partial_\mu + m_0) \chi_\alpha(x), \quad (5.13)$$

where α is the Dirac index. Because the γ matrices have disappeared in favor of

$$\eta_\mu(x) 1 = T^\dagger(x) \gamma_\mu T(x \pm a\hat{\mu}), \quad (5.14)$$

the four components of χ_α decouple, each with the same action. Since the doubling problem implies that there are too many degrees of freedom, one can reduce the total by replacing the four-component field χ_α with a one-component field χ . Just as $\chi_\alpha(\mathbf{p})$ creates $2^4 = 16$ Dirac fermions, $\chi(\mathbf{p})$ creates 16 one-component fermions. Furthermore, the Hamiltonian must be defined from a two-timeslice transfer matrix.

In the continuum limit, one would like to interpret the sixteen fermionic degrees of freedom as four “flavors” of Dirac fermions. This is possible, at least for free fields, but the manipulations involved are too involved to be presented here. These flavors are spread out throughout the lattice, yielding the name “staggered fermions.”

If $m_0 = 0$ the staggered fermion action exhibits a continuous chiral symmetry [8, 9]. After the transformation of eq. (5.11), γ_5 becomes

$$T^\dagger(x) \gamma_5 T(x) = \gamma_5 \varepsilon(x), \quad \varepsilon(x) = (-1)^{n_1+n_2+n_3+n_4}. \quad (5.15)$$

Since the four-component version is identical to naive fermions, the chiral symmetry is the same as always. In the truncation to one-component, one chooses a basis in which γ_5 is diagonal and preserves a $\gamma_5 = +1$ component. Then the chiral symmetry is not lost in passing from a four-component to a one-component field. To be explicit, the one-component action has a continuous $U(1) \times U_\varepsilon(1)$ chiral symmetry

$$\chi(x) \mapsto e^{i\theta + i\alpha\varepsilon(x)} \chi(x), \quad \bar{\chi}(x) \mapsto \bar{\chi}(x) e^{-i\theta + i\varepsilon(x)\alpha}, \quad (5.16)$$

where θ is the parameter of the vector part and α is the parameter of the axial vector part of the symmetry.

Note that $U(1) \times U_\varepsilon(1)$ is only a subset of the full chiral symmetry group that four-flavor QCD must have. Hence, a requirement on staggered lattice QCD is that the chiral-flavor symmetry $SU(4) \times SU(4) \times U(1)$ be restored, in the quantum continuum limit. Nevertheless, the $U(1) \times U_\varepsilon(1)$ chiral symmetry has many important implications. First, when the symmetry is spontaneously broken (e.g. in QCD), there will be a genuine pseudo-Goldstone boson with mass $m_\pi^2 \propto m_0$. In addition, the chiral symmetry constrains the form of physical amplitudes, and the constraints can be derived using the techniques described in Leutwyler’s lectures [10], adapted to $U(1) \times U_\varepsilon(1)$. This is of enormous importance in performing phenomenologically significant calculations with staggered fermions, cf. sect. 10.

The functional integral is specified not only by the action but also by the measure. A fermionic degree of freedoms are represented by Grassman variables. Grassman numbers are numbers that anti-commute, $\{\psi_1, \psi_2\} = 0$. For a single Grassman variable, integration is defined by

$$\int d\psi (\alpha + \varepsilon\psi) = \varepsilon. \quad (5.17)$$

Since $\psi^2 = 0$ more eq. (5.17) contains the most general function of one Grassman variable. Since integration must be invariant under changes of variables, if $\psi = \xi\psi'$, then $d\psi = d\psi'/\xi$. The measure for the fermionic functional integral is $\mathcal{D}\bar{\psi}\mathcal{D}\psi$, where

$$\mathcal{D}\psi = \prod_{x,b} d\psi^b(x), \quad (5.18)$$

and a similar expression for $\mathcal{D}\bar{\psi}$. In eq. (5.18) the index b runs over all indices except space-time, e.g. color, flavor, and spin. If $\psi = \Xi\psi'$ and Ξ is an invertible matrix, then $\mathcal{D}\psi = \mathcal{D}\psi'/\det(\Xi)$.

Exercise 5.2 Suppose the matrix M can be diagonalized. Then show that $\int \mathcal{D}\bar{\psi}\mathcal{D}\psi e^{\bar{\psi}M\psi} = \det(M)$, using the rules for changes of Grassman variables.

6 Lattice Gauge Fields

The goal of this section is to formulate lattice field theories with local gauge invariance. Imagine first that the matter fields are defined on the sites of the lattice, with a gauge field defined on continuous space. The gauge transformation law is, e.g. for fermions,

$$\psi(x) \mapsto g(x)\psi(x), \quad \bar{\psi}(x) \mapsto \bar{\psi}(x)g^{-1}(x), \quad (6.1)$$

where $g(x)$ is an element of (a representation of) the gauge group G . For particle-physics applications G will be a compact, semi-simple Lie group, likely non-Abelian. In the following we shall take $G = \text{SU}(N)$. The equations below follow conventions that the generators T^a are anti-Hermitian ($T^{a\dagger} = -T^a$) and $\text{tr}(T^a T^b) = -\frac{1}{2}\delta^{ab}$. Then the commutator reads $[T^a, T^b] = f^{abc}T^c$.

The kinetic part of the matter-field action arises, in general, from couplings of the form $\bar{\psi}(x)\psi(y)$ where x and y are neighboring sites. These terms are not gauge invariant; instead

$$\bar{\psi}(x)\psi(y) \mapsto \bar{\psi}(x)g^{-1}(x)g(y)\psi(y). \quad (6.2)$$

On the other other hand, the combination $\bar{\psi}(x)U(x,y)\psi(y)$ is gauge invariant if

$$U(x,y) = \text{P exp} \left(\int_x^y dz \cdot A_\mu(z) \right), \quad (6.3)$$

i.e., if $U(x,y)$ is any path-ordered parallel transporter from x to y . It is therefore straightforward to build gauge-invariant lattice models by taking the fundamental gauge degrees of freedom to be the parallel transporters on the links connecting neighbors. Longer parallel transporters can be formed from products of parallel transporters on links.

To write down gauge invariant actions, let us concentrate on hypercubic lattices and write $U_{\pm\mu}(x) = U(x, x \pm \mu a)$. Minimal coupling of gauge fields to matter fields is done by changing the translation operators of the previous sections to covariant translation operators

$$T_\mu = U_\mu t_\mu, \quad T_{-\mu} = \overset{\leftarrow}{U}_{-\mu} t_{-\mu}. \quad (6.4)$$

(Strictly speaking, the representation matrix for U_μ should appear instead of U_μ in this equation.) As with the t_μ , one has $T_{-\mu} = T_\mu^\dagger$, because $U_{-\mu}(x) = U_\mu^\dagger(x - a\mu)$.

The action of the gauge field can be obtained by generalizing the discretization for scalar fields. The following consideration makes it easy. For a local gauge symmetry the full symmetry group is $\mathcal{G} = \prod_x G_x$, a direct product over all sites in the lattice. A matter field $\psi(x)$ transforms non-trivially under G_x and trivially under all other factors. Similarly, a parallel transporter $U(x, y)$ transforms non-trivially under G_x and G_y and trivially under all other factors. Hence, the generalization of the covariant translation operators is to attach to $t_{\pm\mu}$ the representation matrix of \mathcal{G} . Explicitly,

$$T_\mu U_\nu(x) = U_\mu(x) U_\nu(x + a\mu) U_\mu^\dagger(x + a\nu). \quad (6.5)$$

In the continuum the action is a combination of derivative terms and non-linear terms required by gauge invariance. We shall use the covariant translation operators to form a gauge invariant derivative-type term, expecting that the non-linear terms are correct, owing to the gauge invariance. By analogy with eq. (2.12) the derivative terms for U_ν are given by

$$-\sum_{x,\mu} \text{tr}[U_\nu^\dagger(x)(T_\mu + T_{-\mu} - 2)U_\nu(x)] = 2 \sum_{x,\mu} P_{\mu\nu}(x), \quad (6.6)$$

where

$$P_{\mu\nu}(x) = \text{Re tr}[1 - U_\mu(x)U_\nu(x + a\mu)U_\mu^\dagger(x + a\nu)U_\nu^\dagger(x)]. \quad (6.7)$$

Fortunately, the $\mu = \nu$ term vanishes, just as in the continuum, where (for A_ν) the operator $\Delta - \partial_\nu^2$ (no sum on ν) appears. Summing eq. (6.6) over ν yields the gauge invariant lattice action [11]

$$S_G = \frac{\beta}{2N} \sum_{x,\mu,\nu} P_{\mu\nu}(x), \quad (6.8)$$

where β is a parameter related to the bare coupling constant, cf. Exercise 6.1. This action is called the Wilson action, or, to distinguish it from the Wilson fermion action, plaquette action, because the product in eq. (6.7) is parallel transport around a plaquette.

Exercise 6.1 Show that as $a \rightarrow 0$ the plaquette action reduces to the familiar Yang-Mills action $S = (1/4g_0^2) \int d^4x (F_{\mu\nu}^a)^2$, i.e. that the non-linear terms come out correctly. This is a bit tedious, because you must keep terms of $O((aA_\mu)^4)$ in the expansion of U_μ , but it identifies $\beta = 2N/g_0^2$.

The last ingredient of the theory is the functional measure. Lie groups have a natural measure invariant under left (and right) multiplication with a constant,

$$\int dU f(U) = \int d(UV) f(U) = \int dU f(UV^{-1}), \quad (6.9)$$

which is called Haar measure. If the functional measure is defined to be

$$\mathcal{D}U = \prod_{x,\mu} dU_\mu(x) \quad (6.10)$$

i.e. by Haar measure for every link matrix in the lattice gauge field. The invariance property in eq. (6.9) guarantees that $\mathcal{D}U$ is gauge invariant.

7 Lattice Perturbation Theory

Lattice gauge theory has been developed mostly as a tool for non-perturbative calculations. It is also possible to derive perturbation theory on the lattice, but the Feynman rules are not a pretty sight. For QCD (and the Wilson action) a correct set can be found in ref. [12]. For efficient ways of deriving Feynman rules for improved actions (cf. sect. 8) see ref. [13].

There are four important reasons, all related to renormalization, for considering lattice perturbation theory. Because of time limitations, they cannot be considered in detail in these lectures. Instead, we shall summarize the main themes and results, referring the reader to other reviews for further details.

7.1 Reisz' Theorem

Reisz' Theorem, really his series of theorems [14], establishes the equivalence between lattice perturbation theory and traditional approaches [15].

Theorem *If a lattice field theory is renormalizable by power counting, and its propagators exhibit no species doubling, then renormalized perturbation theory is universal, i.e. as $a \rightarrow 0$ it is independent of the lattice action.*

Neither the statement, proof, nor consequences of this theorem are trivial. Unfortunately, because of the high technical level of the proofs, the importance is, perhaps, underappreciated.

In the hypothesis, “power counting” is defined carefully, tailored to the vagaries of lattice Feynman rules. The assumption forbidding species doubling is technical, and it would be helpful to remove the requirement for staggered fermions. In the conclusion, “renormalized perturbation theory” means that renormalized (or physical) couplings are defined, and all other quantities are re-expanded in terms of them. The proof shows that lattice artifacts vanish to all orders in perturbation theory, as $a \rightarrow 0$, for any action whose classical continuum limit is correct.

The proof proceeds by constructing a BPHZ subtraction program, tailored so that counter-terms are local on the lattice. It reveals the first important consequence of Reisz' Theorem. Through BPHZ renormalization, it establishes a link between perturbation theory with a lattice regulator and perturbation theory with dimensional or Pauli-Villars regulators. Since lattice field theory is an approach to quantum field theory that maintains rigorous control over the ultraviolet, this link puts the more familiar perturbative renormalization program on a sounder footing. Those who pursue higher order perturbative calculations should sleep better after studying Reisz' Theorem.

The second important consequence also concerns the renormalization program. Wilson's abstract ideas on the renormalization group bear little resemblance to the traditional, perturbative renormalization group. The abstract ideas have a concrete realization through lattice field theory. Reisz bridges the last gap—showing in detail how to carry through the traditional BPHZ program on the lattice.

7.2 Asymptotic Scaling

Perturbation theory also plays a crucial role in understanding numerical results from Monte Carlo simulations of lattice QCD. For simplicity, let us consider $SU(N)$ lattice

gauge theory without matter fields. There is only one parameter in the action $\beta = 2N/g_0^2$. A solution of the theory (e.g. numerical) yield a relations

$$aE_i = f_i(g_0^2) \quad (7.1)$$

for every physical quantity. (Any dimensionful quantity can be converted to an energy by raising it to the appropriate power.) As $a \rightarrow 0$, E_i should not change. Differentiating eq. (7.1) with respect to $\ln a$ yields

$$a \frac{d}{da} (aE_i) = aE_i + O(a^\nu) \quad (7.2)$$

for the left-hand-side, and

$$a \frac{df_i}{da} = \frac{df_i}{dg_0^2} a \frac{dg_0^2}{da} = 2 \frac{df_i}{dg_0^2} \beta(g_0^2) \quad (7.3)$$

for the right-hand-side, where $\beta(g_0^2) \equiv dg_0^2/d \ln a^2$. (In the notation of sect. 4 $2\beta(g_0^2) = \psi_{g_0^2}$.) Equating these two expressions and neglecting the $O(a^\nu)$ term yields a differential equation

$$f_i = 2 \frac{df_i}{dg_0^2} \beta(g_0^2). \quad (7.4)$$

The β -function can be expanded in power series $\beta(u) = u^2 \sum_{n=0}^{\infty} \beta_n u^n$, where β_n arises from the $(n+1)$ -th loop of perturbation theory. The first two coefficients do not depend on the regulator, but the rest do. For N colors and N_f flavors the universal coefficients are

$$\beta_0 = \frac{11N - 2N_f}{3(16\pi^2)}, \quad \beta_1 = \frac{34N^3 - (13N^2 - 3)N_f}{3N(16\pi^2)^2}. \quad (7.5)$$

Truncating the β -function at two loops and integrating eq. (7.4) gives

$$E_i = C_i \Lambda_{\text{lat}}, \quad (7.6)$$

where C_i is a constant of integration and

$$\Lambda_{\text{lat}} = \frac{1}{a} \left(\frac{\beta_0 + \beta_1 g_0^2}{\beta_0^2 g_0^2} \right)^{\beta_1/2\beta_0^2} e^{-1/2\beta_0 g_0^2(a)} \quad (7.7)$$

is a standard scale parameter, as in eq. (4.10). The behavior given in eqs. (7.6) and (7.7) is called asymptotic scaling, and the $O(a^\nu)$ terms in eq. (7.2) are called scaling violations.

As usual perturbative QCD predicts eq. (7.7), the evolution with an ultraviolet scale (here $1/a$), but not C_i , the initial condition. The only promising method to compute the C_i is numerically, as explained further in sect. 10. Since everyone feels QCD is correct, an important element of numerical lattice QCD is to test numerical algorithms. The prediction of asymptotic scaling, for g_0^2 small enough, offers a powerful check of the numerical approach.

7.3 Matching Scales and Operators

Perturbation theory is also needed to compare unphysical quantities in different regulator schemes. To be concrete, let us choose lattice and dimensional regulators. The latter is the darling of perturbation-theory mavens; it introduces a mass parameter μ and evaluates Feynman integrals in $n = d - 2\varepsilon$ dimensions. Just as one identifies π/a as the ultraviolet cutoff, we shall write

$$\Lambda^2 = 4\pi\mu^2 \exp\left(\frac{1}{\varepsilon} - \gamma_E\right) \quad (7.8)$$

for dimensional regularization. In a comparison with the lattice, Λ plays the role analogous to π/a . On the other hand, it also plays precisely the role of μ in the $\overline{\text{MS}}$ scheme.

As an example, let us consider the relation between g_0^2 and $g_{\overline{\text{MS}}}^2$. In the one-loop approximation the renormalized coupling is

$$g_R^2(q) = g_0^2(\pi/a) \left[1 + g_0^2(\pi/a) \left(\beta_0 \ln \frac{\pi^2}{a^2 q^2} + c_{\text{lat}} \right) \right] \quad (7.9)$$

in terms of the bare lattice coupling and

$$g_R^2(q) = g_{\overline{\text{MS}}}^2(\Lambda) \left[1 + g_{\overline{\text{MS}}}^2(\Lambda) \left(\beta_0 \ln \frac{\Lambda^2}{q^2} + c_{\overline{\text{MS}}} \right) \right] \quad (7.10)$$

in terms of the $\overline{\text{MS}}$ coupling. q is the renormalization point. The constants c depend on the physical choice of $g_R^2(q)$, e.g. quark-anti-quark scattering at momentum transfer q or the QCD correction to $e^+e^- \rightarrow$ hadrons at center-of-mass energy q . But $c_{\overline{\text{MS}}} - c_{\text{lat}}$ is process independent. Since $g_R^2(q)$ is a physical quantity both regulators must yield the same (experimentally measured) number. Equating the right-hand sides of eqs. (7.9) and (7.10) one obtains

$$\frac{1}{g_{\overline{\text{MS}}}^2(\Lambda)} = \frac{1}{g_0^2(\pi/a)} + \beta_0 \ln \frac{\Lambda^2 a^2}{\pi^2} + c_{\overline{\text{MS}}} - c_{\text{lat}}. \quad (7.11)$$

Explicit calculations [16] yield

$$c_{\overline{\text{MS}}} - c_{\text{lat}} = -\frac{N^2 - 1}{8N} + (0.008204)N + (0.002778)N_f, \quad (7.12)$$

which is -0.3087 for $N = 3$ and $N_f = 0$.

The dominant contribution is $-(N^2 - 1)/8N$, and its origin is easy to understand [17]. A formal but elegant way to derive eq. (7.11) is the background field method, which computes the response of the generating functional to an external field [18]. A Gedanken experiment with classical non-Abelian capacitor plates demonstrates that the calculation is a physical one. An important intermediate step in the background field calculation requires the average action per unit volume. In the $\overline{\text{MS}}$ scheme this vanishes, but on the lattice it does not. In fact, the average plaquette action density is $g_0^{-2} \langle P_{\mu\nu} \rangle = (N^2 - 1)/8N$, to leading order, which is precisely the dominant term on the right-hand side of eq. (7.12).

Eq. (7.11) is usually recast to provide a relationship between the renormalization-group invariant scales of the two regulators. To one loop $g_0^{-2} = \beta_0 \ln(1/\Lambda_{\text{lat}}^2 a^2)$ and $g_{\overline{\text{MS}}}^{-2} = \beta_0 \ln(\Lambda^2/\pi^2 \Lambda_{\overline{\text{MS}}}^2)$, so

$$\Lambda_{\overline{\text{MS}}} = \pi e^{(c_{\text{lat}} - c_{\overline{\text{MS}}})/2\beta_0} \Lambda_{\text{lat}}. \quad (7.13)$$

Because of the sizable average plaquette in $c_{\text{lat}} - c_{\overline{\text{MS}}}$, the ratio $\Lambda_{\overline{\text{MS}}}/\Lambda_{\text{lat}}$ is large. For example, $\Lambda_{\overline{\text{MS}}}/\Lambda_{\text{lat}} = 28.8$ for $N = 3$ and $N_f = 0$.

Another class of examples is given by operators appearing in the operator-product expansion [19]. Generically,

$$A(\tfrac{1}{2}z)B(-\tfrac{1}{2}z) = \sum_n C_n(z)O^{(n)}(0), \quad (7.14)$$

in the weak sense of matrix elements. The coefficient functions $C_n(z)$ are c -numbers containing the singularity structures as $z^2 \rightarrow 0$. The sensitivity to initial and final states resides in the matrix elements of local operators $O^{(n)}$. In a typical application the C_n are calculated in perturbation theory using dimensional regularization, and the $\langle h_f | O^{(n)} | h_i \rangle$ are calculated numerically in lattice field theory. To apply eq. (7.14) one must either re-derive the coefficient functions on the lattice, or convert the lattice matrix element to, say, the $\overline{\text{MS}}$ scheme. If the operator is multiplicatively renormalizable, the procedure is analogous to the relationship between couplings. Writing $Z_{\overline{\text{MS}}}^{(n)} O_{\overline{\text{MS}}}^{(n)} = O_R^{(n)} = Z_{\text{lat}}^{(n)} O_{\text{lat}}^{(n)}$, one-loop perturbation theory yields

$$\langle h_f | O^{(n)} | h_i \rangle_{\overline{\text{MS}}}^{(\Lambda)} = \langle h_f | O^{(n)} | h_i \rangle_{\text{lat}}^{(\pi/a)} \left[1 + g^2 \left(\gamma_n \ln \frac{\pi^2}{\Lambda^2 a^2} + c_{\overline{\text{MS}}}^{(n)} - c_{\text{lat}}^{(n)} \right) \right], \quad (7.15)$$

where the $c^{(n)}$ depend on the states $|h_i\rangle$ and $|h_f\rangle$, but the difference does not. To obtain the $\overline{\text{MS}}$ matrix element for eq. (7.14) one can either set $\Lambda = \pi/a$ and keep the correction factor, or set $\Lambda = (\pi/a) e^{(c_{\overline{\text{MS}}}^{(n)} - c_{\text{lat}}^{(n)})/2\gamma_n}$ so that the correction factor is unity.

8 Improved Actions

In the previous sections lattice action were constructed by using nearest-neighbor differences as approximants to derivatives. The dispersion relations (eqs. (3.18), (5.3), and (5.8)) show that the spectrum is affected at $O(a^2)$. This section re-examines the nearest-neighbor approach and addresses the question, whether, and to what extent, better approximants can be derived [20].

At the classical level the procedure is straightforward and has been used for ages in numerical analysis of differential equations. Instead of writing $\Delta_\mu = (t_\mu + t_{-\mu} - 2)/a^2$ for the μ term in the Laplacian, look for an improvement

$$a^2 \Delta_\mu = c_1(t_\mu + t_{-\mu} - 2) + c_2(t_\mu^2 + t_{-\mu}^2 - 2). \quad (8.1)$$

The quickest way to determine the correct values of the c_i is in momentum space where $t_{\pm\mu} = e^{\pm i a p_\mu}$, and demand that the right-hand side be $a^2 p_\mu^2 + O((\mu)^6)$. This exercise yields $c_1 = 4/3$ and $c_2 = -1/12$. Similarly, the $(ap_\mu)^3$ term cancels in

$$a \partial_\mu = b_1(t_\mu - t_{-\mu}) + b_2(t_\mu^2 - t_{-\mu}^2). \quad (8.2)$$

if $b_1 = 4/7$ and $b_2 = -1/14$. Clearly, this procedure can be extended to high order in ap_μ without much work, and inserting these derivatives into the lattice action will improve it at the classical level. Furthermore, for $d > 1$ improved Laplacians or \not{D} can become not only arbitrary but arbitrarily baroque, when the possibility of higher dimensional paths is fully exploited.

Since gauge interactions are introduced through derivatives by the minimal coupling prescription, one might ask what subtleties arise. For gauge-matter interactions, nothing special happens, except that the translation operators t_μ are replaced by their covariant counterparts T_μ . For pure gauge interactions the c_i differ, because $P_{\mu\nu}$ (cf. eq. (6.6)) is simultaneously a derivative term for U_μ and U_ν . By analogy with eq. (8.1) a candidate improved action is

$$S = \frac{1}{g_0^2} \sum_{\mathbf{x}, \mu, \nu} [c_0 P_{\mu\nu}(\mathbf{x}) + c_1 R_{\mu\nu}(\mathbf{x})], \quad (8.3)$$

where

$$R_{\mu\nu}(\mathbf{x}) = \text{Re tr}[1 - U_\nu(\mathbf{x} - a\mu)U_\mu(\mathbf{x} + a\nu - a\mu)U_\mu(\mathbf{x} + a\nu)U_\nu^\dagger(\mathbf{x} + a\nu)U_\mu^\dagger(\mathbf{x})U_\mu^\dagger(\mathbf{x} - a\mu)]. \quad (8.4)$$

comes from a next-to-nearest neighbor interaction,

$$- \sum_{\mathbf{x}, \mu} \text{tr}[U_\nu^\dagger(\mathbf{x})(T_\mu^2 + T_{-\mu}^2 - 2)U_\nu(\mathbf{x})] = \sum_{\mathbf{x}, \mu} R_{\mu\nu}(\mathbf{x}). \quad (8.5)$$

To determine c_0 and c_1 (at the classical level) it is enough to consider U_μ as the parallel transporters of an Abelian plane wave, e.g. $A_\mu(\mathbf{x}) = b_\mu t^3 e^{ik \cdot \mathbf{x}}$. Then a short calculation shows that $c_0 = 5/3$ and $c_1 = -1/12$.

The classical analysis is inadequate at the quantum level for several reasons. From the renormalization group ideas in sect. 4 one realizes that the real goal of the improvement program is to deduce a trajectory for the quantum continuum limit that is closer to the renormalized trajectory. Recall that an irrelevant coupling $h_I \neq 0$ induces corrections of $O(h_I a^n)$ to continuum values of physical quantities. Of course, the lowest n dominates, and in typical cases $n = 2$ or $n = 1$. Without an exact solution it is not feasible, in practice, to set all irrelevant couplings to zero, but it is still desirable to make them as small as possible. As in eq. (4.1) one must start with a general action, and derive and solve the renormalization group equations. For obvious reasons, the terms in eq. (4.1) will be chosen for calculational convenience (e.g. deriving Feynman rules or computer programming). If the error associated with the approximations in the calculations is ϵ , then the coefficients K_n (or c_i and b_i), chosen so that the irrelevant couplings vanish, will really yield $h_I \sim \epsilon$.

For asymptotically free theories, such as QCD, the classical analysis is a good starting point, because perturbation theory describes the approach to the fixed point. Therefore, the scaling behavior of operators differ from their classical values by perturbatively calculable amounts. In other words, irrelevant couplings can be reduced to $h_I \propto g_0^{2\ell}$, at the ℓ -loop level. A generic lattice action can be written schematically as

$$S = a^4 \sum_{\mathbf{x}} \left(g^2 O_4 + a^2 h_6 O_6 + a^4 h_8 O_8 + \dots \right) \quad (8.6)$$

where the O_n is a continuum operator of (classical) dimension n . Suppose an action has been improved classically to $O(a^2)$, i.e. $h_6 = 0$. At one loop insertions of O_8 generate

effects like those of O_4 and O_6 at tree level. The O_4 -like contribution is compensated by renormalizing g^2 . Let the O_6 -like contribution be $c_{8 \rightarrow 6} h_8 g^2$. Taking $h_8 = -c_{8 \rightarrow 6} h_8 g^2$ (instead of 0) cancels it, i.e. improves the action to $O(g^2 a^2)$.

In light of these complications, it is worth discussing exactly what quantities should be improved. An ambitious goal would be to improve all correlators involving the fundamental fields. A more practical and completely adequate goal is to improve only physical quantities. Defining physical states to have $E \ll \pi/a$, $p \ll \pi/a$, their energies and matrix elements must be improved, even if off-shell Green function are not. This improvement criterion is called “on-shell” improvement [21]. A short consideration shows that composite operators require their own improvement, beyond that of the action (i.e. transfer matrix). Imagine computing the matrix elements by adding a source term to the action. The modified action must be improvement in its own right, say to first order in the source. The improved operator is then the part proportional to the source in the improved, modified action.

In lattice QCD the Wilson fermion action is the simplest and most important candidate for systematic improvement. The pure gauge action is automatically improved (classically) to $O(a^2)$, and symmetry forbids $O(a)$ effects from appeared through renormalization. On the other hand, because the Wilson term is dimension five (multiplied by a), cutoff artifacts appear at $O(a)$. To be explicit, the gauge-boson-fermion vertex is $\gamma_\mu + ap_\mu + O((ap_\mu)^2)$, which leads to $O(a)$ artifacts in scattering states (at tree level) and everything else (beyond tree level).

Consider the naive fermion action $S_{\text{NF}} = -a^4 \sum_x \bar{\psi}(\not{D} + m'_0)\psi(x)$, where $D_\mu = (T_\mu - T_{-\mu})/(2a)$. For low momentum states, the naive action is perfectly fine, and its leading lattice artifact is $O(a^2)$. Let us transform the fields by [22]

$$\psi \mapsto [1 - \frac{1}{4}ra(\not{D} - m'_0)]\psi, \quad \bar{\psi} \mapsto \bar{\psi}[1 + \frac{1}{4}ra(\not{D} + m'_0)]. \quad (8.7)$$

The spectrum does not change, because a change of integration variables does not change the integral. The measure $\mathcal{D}\bar{\psi}\mathcal{D}\psi$ does not change, up to $O(a^2 \not{D}^2)$, and

$$S_{\text{NF}} \mapsto -a^4 \sum_x \bar{\psi}[\not{D} + m_0 - \frac{1}{2}ra\not{D}^2]\psi(x) + O(a^2), \quad (8.8)$$

where $m_0 = m'_0(1 + \frac{1}{2}ram'_0)$. One can replace

$$\not{D}^2 = D_\mu^2 - \frac{i}{2}\sigma_{\mu\nu}[D_\mu, D_\nu] \mapsto O_2 = \Delta - \frac{i}{2}\sigma_{\mu\nu}C_{\mu\nu}, \quad (8.9)$$

again up to $O(a^2 \not{D}^2)$, where $\Delta = \sum_\mu (T_\mu + T_{-\mu} - 2)/a^2$ is the (covariant) lattice Laplacian and $C_{\mu\nu} \approx F_{\mu\nu} + O(a^2)$. For example,

$$C_{\mu\nu} = \frac{1}{8} \sum_{\bar{\mu}=\pm\mu} \sum_{\bar{\nu}=\pm\nu} T_{\bar{\mu}} T_{\bar{\nu}} T_{-\bar{\mu}} T_{-\bar{\nu}} - \text{h.c.} \quad (8.10)$$

Since $\bar{\psi}(\not{D}^2 - O_2)\psi$ is a dimension seven operator, the replacement in eq. (8.9) introduces effects of order $g_0^2 a$ at the one-loop level. The effects can be reduced by adding a dimension five operator other than $\bar{\psi}O_2\psi$, say $(ica/4)\bar{\psi}\sigma_{\mu\nu}C_{\mu\nu}\psi$, where the perturbative series for c starts in $O(g_0^2)$. The beauty of these replacements is that the resulting action

$$S_{\text{IF}} = -a^4 \sum_x \bar{\psi}[\not{D} + m_0 - \frac{ra}{2}O_2 + \frac{ica}{4}\sigma_{\mu\nu}C_{\mu\nu}]\psi(x) \quad (8.11)$$

removes the doubling problem in the same fashion as Wilson fermions, without modifying matrix elements on shell. In fact, to all orders in perturbation theory one can set $r = 1$, so that particles travel forward and anti-particles backward in time, and use c to obtain $O(g_0^2 a)$ improvement.

Another way of interpreting this result is that the Wilson action modifies a sensible action by adding the term $ia\bar{\psi}\sigma_{\mu\nu}F_{\mu\nu}\psi$. Since σ_{0i} is the spin operator, one should expect spin splittings (e.g. $m_\rho - m_\pi$ or $m_p - m_\Delta$) to be inaccurate. In charmonium, numerical simulations show that for $g_0^2 \approx 1$ there is a significant difference between $c = -1$ (Wilson action) and $c = 0.4$ (to account for loop effects) [23]. Moreover, since $C_{\mu\nu}$ involves closed paths, $\bar{\psi}\sigma_{\mu\nu}C_{\mu\nu}\psi(x)$ couples fields *locally* [22].

The above reasoning can also be applied to composite operators of fermion fields, which are studied in phenomenological applications of lattice QCD, cf. subsect. 10.2. However, one must track how the operators transform under eq. (8.7). For example, consider a bilinear:

$$\mathcal{O}_\Gamma = m'_0 \bar{\psi} \Gamma \psi \mapsto \mathcal{O}_\Gamma^I = m_0 \bar{\psi} [\Gamma + \frac{1}{4} r a (\Gamma \not{D} - \overleftarrow{D} \Gamma)] \psi + O(a^2). \quad (8.12)$$

In a calculation with S_{IF} the matrix elements of \mathcal{O}_Γ^I are correct to $O(g_0^2 a)$ [24].

The gauge part of the QCD action can also be improved along analogous lines [21]. Again, there is a free parameter x , like r , that can be set according to a criterion separate from on-shell improvement. The range of x is restricted, in order for the action to have a minimum at $U_\mu(x) = 1$. Since the classically improved actions involve next-to-nearest neighbor interactions, the transfer matrix must be defined over two timeslices. In setting up the transfer matrix [25], one finds a breakdown of positivity of the transfer matrix. There are states with complex eigenvalues of the transfer matrix. Fortunately, the low-lying states are isolated from those unphysical states, and there should be no problem defining the continuum limit.

9 Upper Bound on the Mass of the Higgs Boson

As mentioned in sect. 4, the only known fixed point of the scalar field theory is the perturbative one, at which the continuum limit is “trivial.” Clearly, this assertion must be backed up by a non-perturbative analysis, which this section provides at a pedestrian level. A trivial theory need not be useless. Scalar field theories can be used as effective field theories when (more) fundamental physics is well approximated by scalar fields at energy scales $E \lesssim \Lambda$. If one understood the fundamental physics, the renormalization-group equations would determine its effects at experimentally accessible energies.

The lattice ϕ^4 theory has been analyzed from this philosophy in several papers [26]. Triviality still influences the behavior of the effective field theory. The main result is a bound on the renormalized coupling constant. In the $O(4)$ scalar field theory this results in an upper bound on the mass of the Higgs boson (modified in order $g_{\text{SU}(2)}^2$ by gauge interactions). The single component model is discussed here to avoid subtle complications associated with the Goldstone bosons of the $O(4)$ model. The objective of this section is to keep the calculations as simple as possible, yet still demonstrate that analytical, non-perturbative techniques can lead to important physical results. Numerical work has also played an important role in understanding the validity of the

bound [27], but it is not discussed here, because there is plenty of material on numerical lattice QCD in sect. 10.

A non-perturbative analysis is essential for a simple reason. Perturbation theory in g_0 predicts that it is a marginally irrelevant coupling, which means that $\Lambda e^{-1/bg_0(\Lambda)}$ is constant, where Λ is the ultraviolet cutoff and $b < 0$. In other words, $g_0(\Lambda)$ must increase when Λ does; perturbation theory in g_0 predicts its own downfall.

The non-perturbative analysis presented here naturally uses lattice field theory. As usual, we make the rough identification $\Lambda = \pi/a$. Following ref. [28] we shall write the lattice action as

$$S = -2K \sum_{n,\mu} \varphi_n \varphi_{n+\hat{\mu}} + \sum_n \left(\varphi_n^2 + \lambda(\varphi_n^2 - 1)^2 \right). \quad (9.1)$$

For convenience, φ and n are dimensionless: $\varphi_n = a^{(d-2)/2} \phi(\mathbf{x}) / \sqrt{2K}$ and $n = \mathbf{x}/a$, where d is the space-time dimension. This action reduces to the familiar Euclidean Lagrangian

$$\mathcal{L} = \frac{1}{2} (\partial_\mu \phi)^2 + \frac{1}{2} m_0^2 \phi^2 + \frac{g_0}{4!} \phi^4 + \text{constant} \quad (9.2)$$

in the classical continuum limit.

Exercise 9.1 Verify eq. (9.2), by writing $\phi(\mathbf{x} + \hat{\mu}a) = \phi(\mathbf{x}) + a\partial_\mu \phi(\mathbf{x}) + \frac{1}{2}a^2\partial_\mu^2 \phi(\mathbf{x})$, or by working backwards from eq. (2.14). This procedure will yield relations between the bare parameters (K, λ) and (m_0, g_0) .

In the rest of this section we shall take $d = 4$. Only the mass term and ϕ^4 terms of a general scalar potential are used, because others are strongly irrelevant in perturbation theory. The non-perturbative analysis will give an *a posteriori* justification for neglecting, say, ϕ^6 terms.

Eq. (9.1) has a discrete symmetry $\varphi \mapsto -\varphi$, which is spontaneously broken for large enough K . The phase diagram and perturbative fixed point are shown in fig. 4.

Exercise 9.2 Discuss which range of λ corresponds to a potential with one minimum, and which range corresponds to two minima. (At tree level these correspond to unbroken and broken symmetry, respectively.) In which regime do the parameter values $K \ll 1$, g_0 fixed lie?

At $\lambda = \infty$ the model reduces to the Ising model, which is known to have a second-order phase transition (for $d = 4$) at $K = K_c = 0.074750\dots$

Suppose $K \ll 1$ but λ is arbitrary. Then e^{-S} can be expanded in powers of K . In the jargon of statistical mechanics this is a high-temperature expansion. After expanding, the $d\varphi_n$ integrals factorize; any expectation value is a product of integrals of the form

$$I_m(\lambda) = \int d\varphi \varphi^m e^{-[\varphi^2 + \lambda(\varphi^2 - 1)^2]}. \quad (9.3)$$

If m is odd, the integral vanishes.

Consider the propagator, or two-point correlator,

$$\langle \varphi_{r\hat{\rho}} \varphi_0 \rangle = \frac{1}{Z} \int \prod_n d\varphi_n \varphi_{r\hat{\rho}} \varphi_0 e^{-S}. \quad (9.4)$$

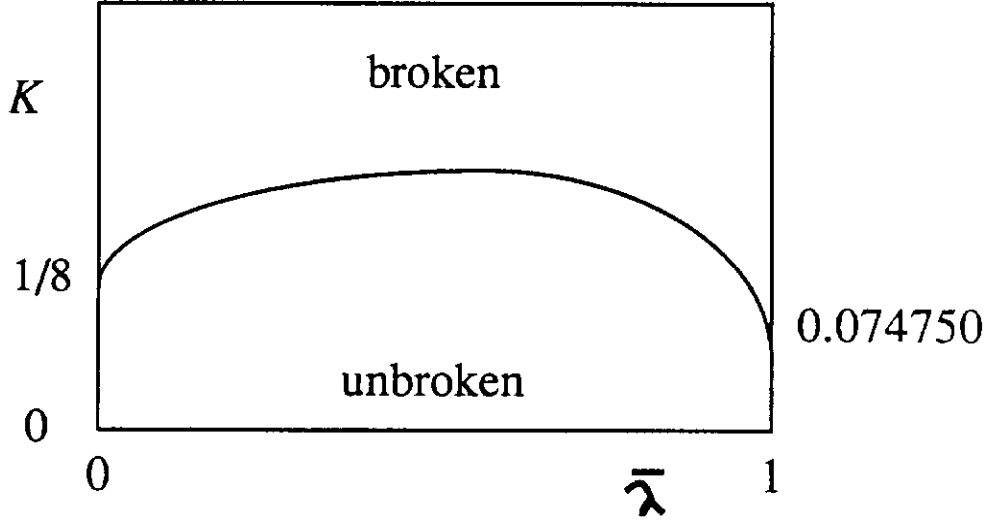


Figure 4: Phase diagram of ϕ^4 theory in four space-time dimensions. At $\lambda = 0$, $K_c = 1/8$; at $\lambda = \infty$, $K_c = 0.074750$.

The term of lowest order in K comes when the expansion of e^{-S} yields a factor of the “hopping term” $2K\varphi_{n+\hat{\rho}}\varphi_n$ for every site n on the straight line linking 0 and $r\hat{\rho}$. One finds

$$\langle \varphi_{r\hat{\rho}}\varphi_0 \rangle = f_2(\lambda) [2K f_2(\lambda)]^r, \quad (9.5)$$

where $f_m(\lambda) = I_m(\lambda)/I_0(\lambda)$; the denominator I_0 comes from the normalization factor Z^{-1} . Eq. (9.5) exhibits the e^{-Ma^r} behavior expected from the transfer-matrix formalism, where the mass is

$$M = -\frac{1}{a} \ln(2K f_2(\lambda)). \quad (9.6)$$

Obviously K and λ must be functions of a , chosen in a suitable way, if M is to stay fixed and finite as $a \rightarrow 0$. Comparing eqs. (3.17) and (9.5) one sees that $\varphi/\sqrt{Z_2}$ is conventionally normalized if

$$Z_2 = 2f_2(\lambda) \text{sh}(Ma) = \frac{1}{2K}, \quad (9.7)$$

the last equality holding for $K \ll 1$.

The renormalized coupling constant is

$$g_R = -\frac{Z_2^4 \langle \varphi_{r\hat{\rho}}\varphi_{-r\hat{\rho}}\varphi_{s\hat{\sigma}}\varphi_{-s\hat{\sigma}} \rangle_c}{Z_2^2 \langle \varphi_{r\hat{\rho}}\varphi_0 \rangle^2 \langle \varphi_{s\hat{\sigma}}\varphi_0 \rangle^2}, \quad (9.8)$$

taking both field normalization and propagator truncation into account. It can also be computed easily. In leading order the numerator has two terms. One comes from a product of hopping terms in towards the origin, yielding $f_4(\lambda)[2K f_2(\lambda)]^{2(r+s)}$. The

other comes from subtracting the disconnected parts, $-3f_2^2(\lambda)[2Kf_2(\lambda)]^{2(r+s)}$. The factors of $2Kf_2(\lambda)$ cancel between numerator and denominator, leaving

$$g_R = \frac{Z_2^2(3f_2^2 - f_4)}{f_2^4} = \frac{2\bar{\lambda}}{(2Kf_2)^2}, \quad (9.9)$$

where $2\bar{\lambda}(\lambda) = 3 - f_4(\lambda)/f_2^2(\lambda)$. When λ is small, $\bar{\lambda} = 3\lambda + O(\lambda^2)$, and as λ increases it rises monotonically to 1. (As $\lambda \rightarrow \infty$, $f_m \rightarrow 1$.)

Exercise 9.3 At $\lambda = 0$, check that eq. (9.6) reproduces eq. (3.18) for $p = 0$ and $K \ll 1$. You will need the result of Exercise 9.1, $2d + m_0^2 a^2 = (1 - 2\lambda)/K$ and $f_2(0) = \frac{1}{2}$. When λ is small, check that eq. (9.9) reduces to the expression for g_0 in Exercise 9.1.

Note that at fixed K , g_R is bounded. The physics behind this result is that the size of the renormalized coupling measures the extent of the field fluctuations. This fact is usually obscured by normalizing the field to a conventional size. In the normalization of eq. (9.1), however, a strong $\lambda\varphi^4$ interaction suppresses fluctuations; in the Ising limit, $|\varphi|$ does not fluctuate at all. Indeed, the essence is captured by a single degree of freedom, for which the expectation value of φ^m is $f_m(\lambda)$.

To apply these lattice results to continuum physics, one must accurately determine the location of the critical line in fig. 4, and then compute g_R close enough to it, so that effects of order M/Λ are not too large. Lüscher and Weisz [28] have done both by applying the tenth-order high-temperature expansion [29]. The critical line is determined by pin-pointing where the series diverges. For K too close to K_c the expansion is no longer accurate, but for $K \leq 0.95K_c$ it still is. On the line $K = 0.95K_c$ the renormalized coupling is bounded, as suggested in eq. (9.9). The Ising limit, $\lambda = \infty$, yields the maximal value $g_{R, \max} = 41$, which is “small,” because the natural expansion parameter of renormalized perturbation theory is $g_R/16\pi^2$. (The leading order expression in eq. (9.9) is only qualitatively correct, estimating $g_{R, \max} = 99$.) The line $K = 0.95K_c$ has other admirable features, in particular, $a^{-1} \lesssim 2M$, i.e. the scale of new physics Λ is not much larger than M itself.

Since g_R is small, one can integrate perturbative renormalization group equations, to study the strip of the phase diagram with $0.95K_c \leq K \leq K_c$. Given the form of the initial data, $a(0.95K_c, \lambda)$ and $g_R(0.95K_c, \lambda)$, it is easier to work on curves of constant λ than curves of constant physics. Then it follows immediately that g_R vanishes on the critical line. The continuum limit is trivial. Furthermore, since renormalized perturbation theory is universal (Reisz’ Theorem) changes in the initial lattice action would not alter this step of the analysis.

These calculations are done in the unbroken phase, so they do not apply directly to the Higgs boson. However, it is possible to transfer the results across the critical line, into the broken phase using perturbation theory in $\Delta K = K - K_c$. Again the renormalized coupling is bounded, $g_R \leq g_{R, \max}$. In the region where $am_H \leq 0.5$ (m_H is the Higgs boson mass), $g_{R, \max} = 48$. In terms of the Higgs-field vacuum expectation value $v = 250$ GeV, $g_R = 3m_H^2/v^2$, so the bound on g_R is a bound on m_H . Hence, $m_H \lesssim 1$ TeV if the cutoff $\Lambda = 2\pi m_H \approx 6$ TeV. If Λ/m_H is higher, $g_{R, \max}$, and hence $m_{H, \max}$, is smaller.

There are only two ways to raise the bound on m_H . One is to fiddle with the lattice action, which boils down to making specific assumptions about the effective

action at scale Λ . An action different from eq. (9.1) would provide different the initial conditions for the perturbative renormalization group equations, perhaps leading to a larger $g_{R, \max}$ in the Higgs phase. It might also provide other physics implications—signs of new physics. The other way to raise the bound is simpler: merely lower Λ/m_H . But then there will almost certainly be signs of new physics. If the experiments are precise enough, these would be seen in the 1 TeV region.

These results apply only to the one-component ϕ^4 theory. Lüscher and Weisz have, however, repeated the whole analysis for the $O(4)$ scalar field theory [30]. Every feature follows through as above, although the details are more demanding. Furthermore, numerical work [27] confirms the analytical results. The result for the Higgs boson mass is a bit stronger, $m_H \lesssim 630$ GeV. Even allowing a conservative margin of error (for theorists fiddling with and experimentalists detecting m_H/Λ effects), the conclusion remains compelling: *either* a fundamental Higgs boson *or* new physics will be found at an energy scale below 1 TeV.

10 Numerical Calculations

With the theoretical foundations and one analytical example of non-perturbative techniques out of the way, this section covers numerical analysis of the functional integral, focusing on QCD. It does *not* give details of the computation-intensive algorithms. Instead, in line with the goal of providing a guide to non-experts, it points out some of the big obstacles, and tries to cultivate an intuition for numerical analysis well done. Consumers of lattice QCD calculations need to recognize the difference between solid and shabby results.

For non-zero a and finite N_μ lattice field theory is defined by a multi-dimensional integral. The suggestion is to use a computer and “Just do it.” For bosonic degrees of freedom, such as the gauge field in QCD, the only viable option is Monte Carlo integration with importance sampling [31]. Let $U^{(i)}$ represent a gauge-field configuration, i.e. a random $SU(N)$ matrix for each integration variable $U_\mu(\mathbf{x})$. Imagine generating a large ensemble of configurations $\{U^{(i)}\}$, $i = 1, \dots, N_{\text{conf}}$, distributed according to the product Haar measure $\mathcal{D}U = \prod_{\mu, \mathbf{x}} dU_\mu(\mathbf{x})$. A numerical estimate of an expectation value would be

$$\langle f(U) \rangle = \frac{1}{Z} \int \mathcal{D}U f(U) e^{-S(U)} \approx \frac{1}{N_{\text{conf}}} \sum_{i=1}^{N_{\text{conf}}} f(U^{(i)}) e^{-S(U^{(i)})}, \quad (10.1)$$

where N_{conf} is the size of the ensemble. This is a garden-variety Monte Carlo integration algorithm. Because S is extensive, it is hopelessly inefficient. For a large lattice e^{-S} varies over extremely many orders of magnitude. However, as long as $e^{-S} > 0$ for all configurations, which is usually the case, there is an alternative. Suppose a configuration $U^{(i)}$ appears in the ensemble with probability $\mathcal{D}U e^{-S(U^{(i)})}$. This is importance sampling. Then the numerical estimate is

$$\langle f(U) \rangle \approx \overline{f(U)} \equiv \frac{1}{N_{\text{conf}}} \sum_{i=1}^{N_{\text{conf}}} f(U^{(i)}). \quad (10.2)$$

Several suitable algorithms are available for gauge theories, taking the Haar measure correctly into account. An ensemble generated by importance sampling provides an

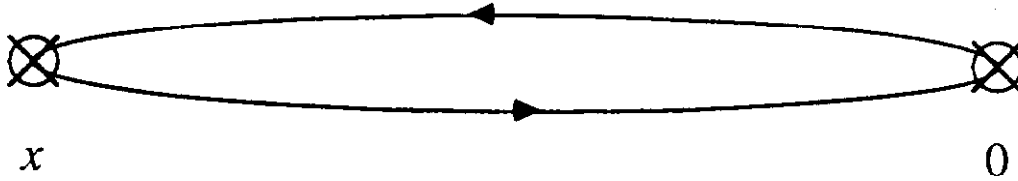


Figure 5: Quark-line diagram for the pion propagator.

estimate \bar{f} for every $\langle f \rangle$, leading to the slightly imprecise terminology “Monte Carlo simulation.”

Fermion fields, such as the quarks in QCD, cannot be handled this way, because they take values in a Grassman algebra. A general fermion action can always be written in the form $\bar{\psi}M(U)\psi$, where $M(U)$ is a matrix function of the boson fields U with space-time, spin and internal indices. The fermion fields can then be integrated exactly:

$$\int \mathcal{D}U \mathcal{D}\psi \mathcal{D}\bar{\psi} e^{-S(U) + \bar{\psi}M(U)\psi} = \int \mathcal{D}U \det M(U) e^{-S(U)}, \quad (10.3)$$

$$\int \mathcal{D}U \mathcal{D}\psi \mathcal{D}\bar{\psi} \psi_i \bar{\psi}_j f(U) e^{-S(U) + \bar{\psi}M(U)\psi} = \int \mathcal{D}U M_{ij}^{-1} f(U) \det M(U) e^{-S(U)}, \quad (10.4)$$

and similar expressions for expectation values of products of fermion fields. The computation of determinant or inverse of M requires overwhelming amounts of computer time. Fortunately, almost every problem in QCD can be re-cast into a system of linear equations. Writing space-time indices explicitly, but spin and internal indices implicitly, one must solve

$$M(x, y)G_\chi(y) = \chi(x) \quad (10.5)$$

for G_χ , which is the lattice analog of the Dirac equation in a background boson field. If $\chi(x) = \delta(x - z)$, then $G_{\delta_z}(y) = G(y, z)$ is the fermion propagator from z to y , including all interactions with the boson fields. By linearity, $G_\chi(y) = \sum_z G(y, z)\chi(z)$. The dimension of M is huge, but, because the interactions are local, it is sparse—most of its entries are zero, and there are several acceptable algorithms for solving systems such as eq. (10.5) for sparse matrices.

The propagators make it easy to generalize eq. (10.4) to arbitrary products of fermion fields. Under the bosonic functional integral they are replaced by propagators according to Wick’s theorem. This leads to a diagrammatic notation. For example, a π^+ meson correlator $\langle \bar{d}\gamma_5 u(x) \bar{u}\gamma_5 d(0) \rangle$, where u and d are up and down quarks, is sketched in fig. 5. One should keep in mind that the gauge-field average is implied in fig. 5; it represents the sum of all Feynman diagrams with gluons and internal quark loops attached.

If $\det M(U)e^{-S(U)}$ is positive for all U configurations, it can be used as a probability distribution. In lattice QCD, $\det M$ is positive for staggered fermions⁶ or for two equal-mass flavors of Wilson fermions. All “full QCD” algorithms being used nowadays start

⁶Recall, one staggered Fermi field yields 4 flavors in the continuum limit.

by expressing $\det M$ as a bosonic functional integral [32]:

$$\det M(U) = \int \mathcal{D}\phi \exp \left[-\phi^\dagger M^{-1}(U)\phi \right] = \int \mathcal{D}\phi e^{-S_\phi(\phi,U)} \quad (10.6)$$

and generating ϕ - U configurations with weight $e^{-S(U)-S_\phi(\phi,U)}$. In lattice QCD the present algorithm of choice is called “hybrid Monte Carlo” [33]. Wise-guys have observed that all fields of numerical science proceed until an algorithm is given this name. Time will tell if algorithms for lattice QCD have indeed reached their apex.

An alternative is the quenched (or valence) approximation, which approximates $\det M(U)$ by a constant, independent of U , and a compensating shift in the bare parameters [34]. In terms of quark-line diagrams $\det M$ produces internal fermion loops. Hence, the shift in the bare parameters ought to account well for high-momentum loops, but not for low-momentum loops. Operationally, the gauge fields are generated according to the pure gauge theory weight $e^{-S(U)}$. Hadron correlators can still be computed, though, using fermion propagators á la eq. (10.5) for the valence quarks. Algorithms for quenched QCD are much, much faster than those for full QCD. In hybrid Monte Carlo most of the computer time in generating the ensemble $\{U^{(i)}\}$ is spent solving eq. (10.5) with the (dynamical) field ϕ in eq. (10.6) as a source. A quenched simulation generates a pure gauge ensemble and must cope with eq. (10.5) only for valence quark propagators.

The Monte Carlo procedures lead to statistical errors. Owing to the central limit theorem (the law of large numbers), the estimates \bar{f} are Gaussian distributed with variance

$$\sigma_{\bar{f}}^2 = \frac{1}{N_{\text{conf}} - 1} (\langle f^2 \rangle - \langle f \rangle^2), \quad (10.7)$$

which can be estimated by $(\overline{f^2} - \bar{f}^2)/(N_{\text{conf}} - 1)$. A more subtle problem arises when several averages \bar{f}_i must be combined to obtain a physical result. For example, the mass comes from a fit of the time-dependence of eq. (3.24). Then the statistical error analysis must take into account that

$$\sigma_{\bar{f}_1 \bar{f}_2}^2 = \frac{1}{N_{\text{conf}} - 1} (\langle f_1 f_2 \rangle - \langle f_1 \rangle \langle f_2 \rangle) \neq 0. \quad (10.8)$$

In other words, the data that come out of a simulation are correlated, often strongly. Estimates of uncertainties that neglect these correlations can be either too large or too small. For example, in subsect. 10.2 we shall see that ratios frequently have smaller statistical uncertainties than numerator or denominator separately.

It is not enough to “just do it.” Instead, “do it over and over,” to study the lattice-spacing and volume dependence. To decouple the two, it is best to study one while holding the other fixed. The volume dependence is reasonably straightforward to attack: fix the bare couplings (and hence a) and vary the lattice size N_μ . Usually this is done by fixing the geometry, say $N_i = N_{\text{space}}$ and $N_t = 2N_{\text{space}}$ so there is only one parameter to vary. The lattice-spacing dependence is more problematic, because both the bare couplings and N_{space} must be varied, such that the physical size of the box $L_{\text{space}} = aN_{\text{space}}$ stays fixed, cf. eq. (2.7). Perturbation theory controls the scaling behavior in QCD, so the adjustments can be made on that basis, at least close enough to the continuum limit. Obtaining reliable estimates of lattice-spacing and finite-size

uncertainties is similar to the analysis of systematic errors in experiments. In the end, every piece of physical or mathematical information from outside the simulation ought to be used to check that the numbers make sense. Fortunately, theoretical considerations predict the form of both the a dependence (at small a) and the L dependence (at both small and large L).

Let us review what is known about the lattice spacing dependence. At the continuum limit ratios aE_i/aE_1 become independent of a —they scale—up to scaling violations of $O(a^n)$. Eventually the scaling violations are negligible, and then the energies should obey asymptotic scaling, possibly at the more-than-two-loop level. Before scaling sets in, one can remove the violations by extrapolation. The check of asymptotic scaling can be approached either by brute force with larger lattices at smaller values of g_0^2 , or by improving the action so that scaling violations are truly negligible. The real problem is choosing the fiducial quantity E_1 to define a . In full QCD there are $N_f + 1$ free parameters, and therefore $N_f + 1$ physical quantities must be taken from experiment. Since the hadron masses are sensitive to the quark masses, a possible procedure is to tune the quark masses so that N_f hadron mass ratios are correct. Then a is merely a conversion factor from lattice ($a = 1$) to physical (e.g. GeV) units. In numerical simulations this approach is annoying, especially when one starts worrying about holding the physical volume fixed. In practice it is easiest to monitor scaling behavior if E_1 is insensitive to the quark masses. Fortunately there is a good choice [17], which will be discussed further in subsect. 10.3.

A full discussion of the L dependence is well beyond the scope of these lectures. (The lattice is not essential in obtaining the results.) In the small L limit a perturbative expansion in $\alpha_{\overline{\text{MS}}}(1/L)$ can be used to integrate out the gauge field, except for its constant modes. The constant modes constitute a quantum-mechanics problem that is non-trivial but still simpler than field theory. In the large L limit one can assume that the long-distance structure is described by a massive effective field theory. Stronger effects of Goldstone bosons can be incorporated using the techniques of chiral perturbation theory. In either case, the effective field theory can be formulated in a finite volume, leading to general formulae for finite-size effects. The unknowns in the formulae are simply related to couplings in the effective field theory, so the formulae give not only a prescription for extrapolating, but also a method to compute these couplings.

Combining data from the computer with other information is the most arduous task in computational physics. It is also the most important. Unfortunately, systematic uncertainties can only be fully analyzed when statistical errors are small enough. Since it requires less computer time, most numerical work with high enough statistics to study lattice-spacing, and volume uncertainties has been done in the quenched approximation. Obviously, the quenching introduces a yet another systematic error. For many properties of light hadrons this is not easy to estimate, because there is little hard information besides the quenched simulations themselves. One possibility is to examine chiral models, asking which contributions can or cannot appear in the quenched approximation [35]. A recent variation on this theme is to develop effective Lagrangians directly for quenched QCD [36]. From these and other considerations there are good indications that quenching is under control for heavy-quark systems, subsect. 10.3, and for some ratios of matrix elements, subsect. 10.2. These calculations, therefore, warrant serious attention, and they are discussed in detail below.

The remainder of this section is divided into three parts. Subsect. 10.1 describes the bread-and-butter topic of mass spectroscopy. The emphasis is on ways to improve the spectrum until it serves as a serious test of QCD. Subsect. 10.3 describes an application of the charmonium spectrum to compute the running coupling constant of QCD, $\alpha_{\overline{\text{MS}}}(5 \text{ GeV})$. Finally, the steps in the calculation of the “bag parameter” of the kaon system are presented in subsect. 10.2.

10.1 Spectroscopy

The first step in a calculation of the mass spectrum is to classify the states according to the symmetries of the transfer matrix. The quantum numbers associated with translations are the momentum. The rest of the classification is too tedious to give in detail, but the Review of Particle Properties tells us what to expect: mesons and baryons labeled by J^{PC} , isospin, strangeness, etc. Assuming a hypercubic lattice of size $N_{\text{space}}^3 \times N_t$ with periodic (anti-periodic) boundary conditions for gauge fields (fermions), both the lattice and the finite box both break some of the rotational symmetries. There are only finitely many representations instead of one for each integer J . Multiplets with high angular momentum must appear as “accidental” degeneracies in the continuum and large volume limits.

In addition, there are glueballs, states that can be constructed out gluons only, labeled by J^{PC} . None has been unambiguously identified in experiments. If J^{PC} is accessible in the quark model a glueball is an idealization, because it can mix with flavor singlet $q\bar{q}$ states. In the following, distinctions between “glueballs” and “normal mesons” are made with this idealization in mind. There are combinations of J^{PC} that cannot appear in the quark model; these are called exotics or oddballs.

The spectrum is extracted from the time dependence of correlation functions. Let $\hat{\Phi}_r$ denote an operator annihilating states with quantum numbers $r = \{J^{PC}, p, \dots\}$. From eq. (3.24)

$$C_r(t) = \langle \hat{\Phi}_r(t) \hat{\Phi}_r^\dagger(0) \rangle = \quad (10.9)$$

$$\sum_{\beta} |\langle 0 | \hat{\Phi}_r | \beta, r \rangle|^2 e^{-tE_{\beta,r}} + \sum_{\beta} |\langle 0 | \hat{\Phi}_r^\dagger | \beta, r^* \rangle|^2 e^{-(T-t)E_{\beta,r^*}},$$

where r^* is the complex-conjugate representation and t/a is defined modulo $T/a = N_t$. In QCD, r is real for zero-momentum mesons and glueballs, but not for baryons. If $p = 0$ the energy $E_{\beta,r}$ is a mass, and the objective is to exploit the exponential fall-off to compute the low-lying ones for each r . The coefficients $|\langle 0 | \hat{\Phi}_r | \beta, r \rangle|^2$ depend on the choice of operator, but (for given r) the energies $E_{\beta,r}$ do not.

To compute the mass of the lowest-lying state one proceeds as follows. One must identify a region $t_{\min} \leq t \leq t_{\max}$ where one state dominates, so that

$$C_r(t) = |\langle 0 | \hat{\Phi}_r | 1, r \rangle|^2 e^{-tE_{1,r}} \quad (10.10)$$

for $r \neq r^*$, or

$$C_r(t) = |\langle 0 | \hat{\Phi}_r | 1, r \rangle|^2 (e^{-tE_{1,r}} + e^{-(T-t)E_{1,r}}) \quad (10.11)$$

for $\tau = \tau^*$. A convenient diagnostic for this region is the effective mass

$$m_f(t + \frac{1}{2}a) = \frac{1}{a} \ln \left(\frac{C_r(t)}{C_r(t+a)} \right), \quad (10.12)$$

which should be t -independent in the interval $t_{\min} \leq t \leq t_{\max}$. The spectrum does not depend on Φ_r , which should be chosen to minimize t_{\min} , because the signal-to-noise ratio C/σ deteriorates with t . This phenomenon is seen in Monte Carlo data. It can also be analyzed by field theoretic techniques, because $\langle f^2 \rangle$ is just another correlator. Although the choice of operator is a technical issue, all calculations in lattice QCD are vastly improved by finding good ones. Therefore, the next several paragraphs review the signal-to-noise ratio and survey techniques for increasing it.

Glueball operators are functions of the gauge field, so eq. (10.7) can be applied immediately. The variance of (the estimate of) $C_r(t)$ is

$$\sigma_r^2(t) = \frac{1}{N_{\text{conf}} - 1} \left(\langle \Phi_r(t) \Phi_r^\dagger(0) \Phi_r(0) \Phi_r^\dagger(t) \rangle - C_r^2(t) \right). \quad (10.13)$$

For simplicity, suppose that τ does not have vacuum quantum numbers. (When it does, the analysis is complicated by subtracting the vacuum's contribution out of $C_r(t)$.) According to the transfer matrix formalism, the first term in eq. (10.13) is given by eq. (3.24) with $\mathcal{O}_1 = \mathcal{O}_2 = |\Phi_r|^2$. The quantum numbers of the states created by $|\Phi_r|^2$ are $\tau \oplus \tau^*$, which always contains the vacuum. Hence the vacuum dominates the spectral sum $\langle \Phi_r(t) \Phi_r^\dagger(0) \Phi_r(0) \Phi_r^\dagger(t) \rangle \approx \langle \Phi_r(t) \Phi_r^\dagger(t) \rangle \langle \Phi_r(0) \Phi_r^\dagger(0) \rangle$. Hence,

$$\sigma_r^2(t) \approx \frac{C_r^2(0)}{N_{\text{conf}} - 1}, \quad (10.14)$$

and the signal-to-noise ratio is

$$\frac{\text{SIGNAL}}{\text{NOISE}} = \frac{C_r(t)}{C_r(0)} \sqrt{N_{\text{conf}} - 1}. \quad (10.15)$$

Since $C_r(t)$ falls exponentially in t and $C_r(0)$ does not, the risk is that statistical errors become intolerable before the plateau in m_f appears. Furthermore, $C_r(0)$ grows as $a \rightarrow 0$ for local operators, making the continuum limit inaccessible, whereas non-local operators can solve this problem [37].

Exercise 10.1 Generalize eq. (10.14) to show that fluctuations in $C_r(t_1)$ and $C_r(t_2)$ are correlated with variance (cf. eq. (10.8))

$$\sigma_r^2(t_1, t_2) \approx \frac{C_r(0) C_r(|t_1 - t_2|)}{N_{\text{conf}} - 1}. \quad (10.16)$$

For quark-model states the analysis differs because propagators are used. Consider an isospin 1 meson, for example, with $\Phi_r = \bar{d} \Gamma_r u$, where Γ_r is a γ matrix, and u and d are Wilson fermion fields for the up and down quarks. To compute the meson correlator, one first computes quark propagators and then works out

$$C_r(t) = - \sum_{\mathbf{x}} \langle \bar{d} \Gamma_r u(\mathbf{x}) \bar{u} \Gamma_r^\dagger d(0) \rangle = \sum_{\mathbf{x}} \langle \text{Tr} \{ \Gamma_r G^{(u)}(\mathbf{x}, 0) \Gamma_r^\dagger G^{(d)}(0, \mathbf{x}) \} \rangle \quad (10.17)$$

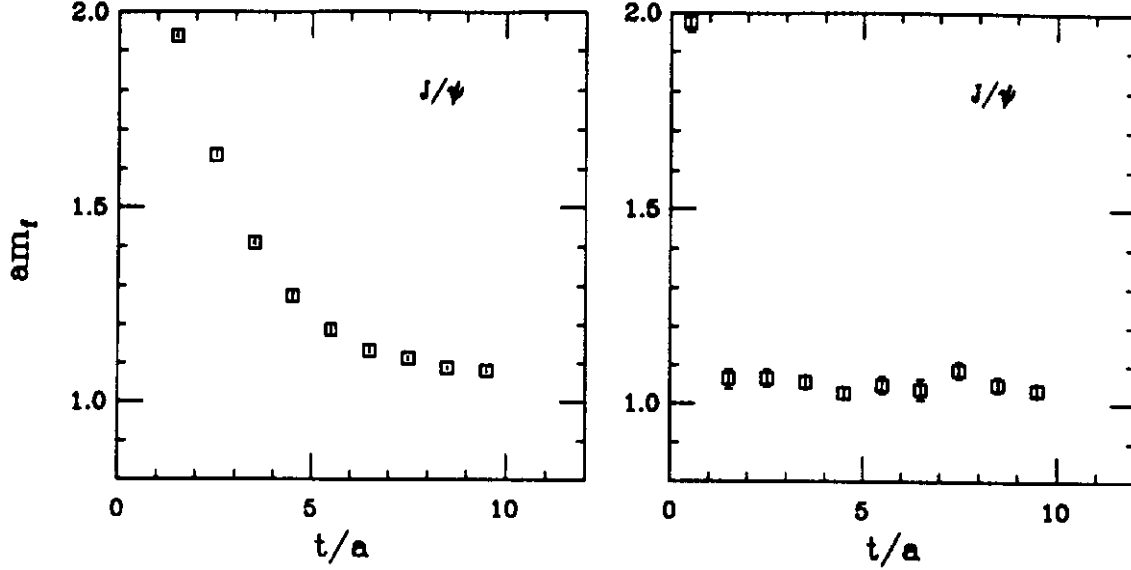


Figure 6: Effective mass plots for the J/ψ with (a) point-like and (b) non-local operators.

where the average in the last line is over the gauge fields only. The variance of this object is given by

$$\sigma_r^2(t) = \frac{1}{N_{\text{conf}} - 1} \left(\sum_{\mathbf{x}} \sum_{\mathbf{y}} \langle \text{Tr} \{ \Gamma_r G^{(u)}(\mathbf{x}, 0) \Gamma_r^\dagger G^{(d)}(0, \mathbf{x}) \} \times \right. \quad (10.18)$$

$$\left. \text{Tr} \{ \Gamma_r G^{(u)}(0, \mathbf{y}) \Gamma_r^\dagger G^{(d)}(\mathbf{y}, 0) \} \rangle - C_r^2(t) \right),$$

where $x_4 = y_4 = t$. The quark-line diagram for σ_r^2 has four quark lines in it. The lowest-energy of states with four quarks is approximately $2m_\pi$. For t large enough $\sigma_r^2(t) \propto e^{-2m_\pi t}$, and the signal-to-noise ratio

$$\frac{\text{SIGNAL}}{\text{NOISE}} \propto \frac{e^{-m_1 t}}{e^{-m_\pi t}} \sqrt{N_{\text{conf}} - 1}, \quad (10.19)$$

where m_1 is the lowest-lying state created by $\bar{d}\Gamma_r u$. Unless $m_1 = m_\pi$, this signal-to-noise ratio also falls with t , although not as severely as with glueballs.

The signal-to-noise ratio shows that it is imperative to find an operator that has t_{min} as small as possible. Point-like operators (including those that become point-like as $a \rightarrow 0$) have proven inadequate. Fig. 6a shows an example effective-mass plot for J/ψ mesons, using a point-like operator $\bar{c}\gamma_3 c$. Clearly, the point-like operator's amplitude to create higher-lying states is too high. Consequently, there is a steep decrease in m_f in fig. 6a as states with energies $E \sim \pi/a$ die off. A better choice would be a non-local operator, with "size" close to that of the J/ψ meson.

A heuristic approach is that just about any operator with the right size should do. Define a “smeared” quark field by iterating

$$\tilde{\psi}(\mathbf{x}) = \psi(\mathbf{x}) + \alpha \sum_{i=1}^3 (T_i + T_{-i} - 2)\psi(\mathbf{x}) \quad (10.20)$$

for suitable α . Because the covariant translation operators T_i appear in eq. (10.20), $\tilde{\psi}$ gauge transforms as ψ . The sum in eq. (10.20) runs over space-like directions only, so that correlators built with $\tilde{\psi}$ are local in time and, hence, compatible with the transfer matrix.

Exercise 10.2 For free field theory, show that M iterations of eq. (10.20) lead to

$$\tilde{\psi}(\mathbf{p}) = (1 - a^2 \alpha \hat{\mathbf{p}}^2)^M \psi(\mathbf{p}) \quad (10.21)$$

in momentum space. Hence, if $M \rightarrow \infty$ as $a \rightarrow 0$ with $Q^{-2} = M\alpha a^2$ fixed, then $\tilde{\psi}(\mathbf{p}) = e^{-\hat{\mathbf{p}}^2/Q^2} \psi(\mathbf{p})$. In coordinate space $\tilde{\psi}(\mathbf{x}, t) = \sum_{\mathbf{y}} g(\mathbf{x} - \mathbf{y}) \psi(\mathbf{y}, t)$, where $g(\mathbf{x})$ is a periodic function similar to a Gaussian.

Because it has an extent of size $1/Q$, the operator $\tilde{\psi}(\mathbf{x})\Gamma\tilde{\psi}$ should couple strongly to low-lying states. For glueballs the analog of eq. (10.20) does in fact yield much improved results. However, a drawback is that a smeared operator might well create low-lying states other than the *lowest*-lying one, either because Q is poorly chosen, or because a Gaussian is a poor shape.

Exercise 10.3 Consider the meson correlator $\langle \Phi(\mathbf{x})\Phi^\dagger(0) \rangle$, where $\Phi(\mathbf{x}) = \bar{d}(\mathbf{x})\Gamma\bar{u}(\mathbf{x})$, i.e. up is smeared and down is not. Work out what sources χ are needed for the quark propagators.

In the non-relativistic limit, the smeared field creates a two-particle state with a harmonic oscillator wave function. If the quark mass is not too light, one might consider using a wave function from a phenomenologically successful potential instead. Even for light hadrons, the appalling success of the non-relativistic quark model suggest that these wave functions should make a good start. These wave functions are defined for a choice of gauge, for example Coulomb gauge. A lattice version of Coulomb gauge [39] is obtained by finding the gauge transformation g that minimizes

$$\mathcal{F}_C = \sum_{\mathbf{x}, i=1}^3 \text{Re}[1 - \text{Tr}^g U_i(\mathbf{x})]. \quad (10.22)$$

In the naive continuum limit $\mathcal{F}_C \propto \int A^2$, which has extrema for $\nabla \cdot \mathbf{A} = 0$. Once the ensemble of gauge fields has been brought into Coulomb gauge, a wide variety of operators

$$\Phi_{\Gamma, f}(\mathbf{x}) = \sum_{\mathbf{y}} \tilde{\psi}(\mathbf{x})\Gamma\psi(\mathbf{y})f(\mathbf{x} - \mathbf{y}), \quad (10.23)$$

where $x_4 = y_4$, can be constructed. A good way to determine f is to compute the ratio

$$f(\mathbf{x}) = \frac{\langle \tilde{\psi}(\mathbf{x}, t)\Gamma\psi(\mathbf{0}, t)\Phi(0) \rangle}{\langle \tilde{\psi}(\mathbf{0}, t)\Gamma\psi(\mathbf{0}, t)\Phi(0) \rangle}, \quad (10.24)$$

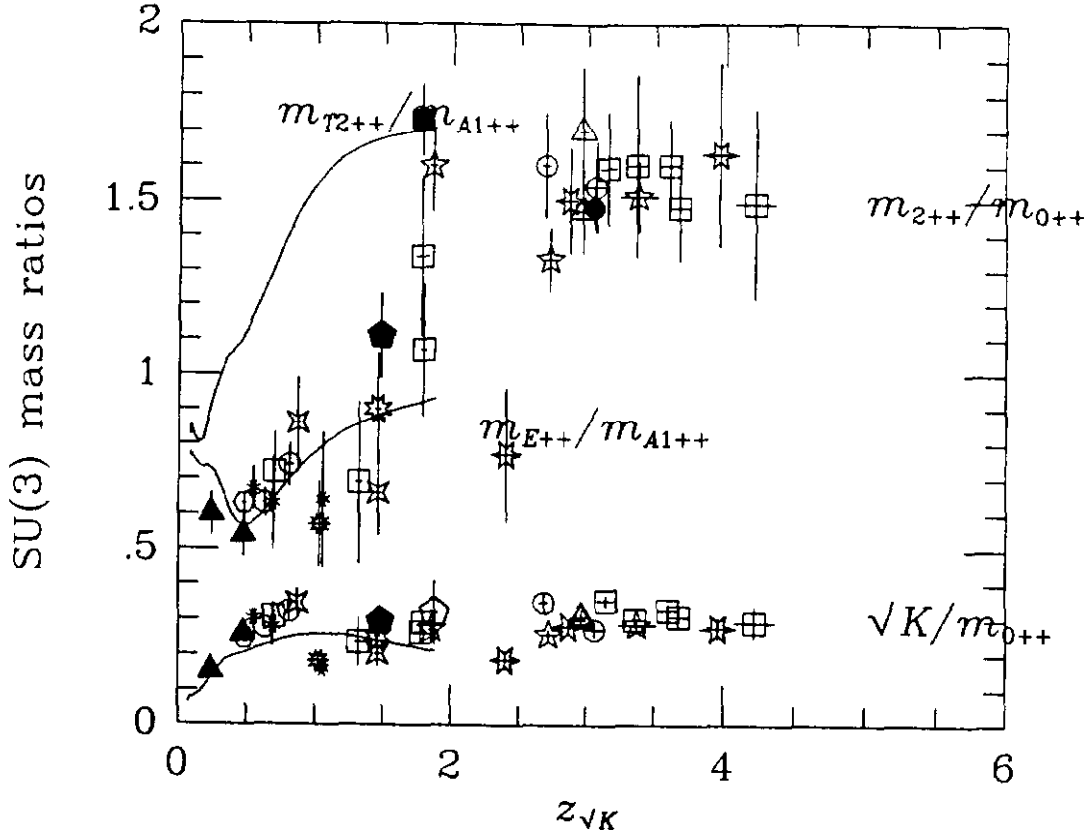


Figure 7: Plot of SU(3) glueball mass ratios vs. $z\sqrt{K}$.

where Φ is an acceptable operator, for large enough t to project onto the lowest-lying state. Using a fit to $f(\mathbf{x})$ to the form $e^{-Q|\mathbf{x}|}$, fig. 6b shows the effective mass for J/ψ . It is independent of t for $2 \leq (t/a) \leq 10$.

Once an effective-mass plateau has been identified, the masses should be computed by fitting the numerical data for $C_r(t)$ to the functional form on the right-hand side of eq. (10.10) or eq. (10.11). As we have emphasized above, this must be done taking correlations in the errors into account. Then the fit “averages” the information with the correct weight. In addition to an estimate of the mass, the best fit yields estimates of the (statistical) uncertainty and the goodness-of-fit. The latter two are especially sensitive to correlations in the errors. Since they measure the reliability of numerical results, questions of systematic errors and physical interpretation cannot be answered unless they are determined correctly.

Fig. 7 gives a summary of Monte Carlo results of glueball masses in the pure gauge theory with gauge group SU(3). It plots mass ratios as a function of $z\sqrt{K} = N_{\text{space}}a\sqrt{K}$, where $K = (420 \text{ GeV})^2$ is the string tension. Hence, $z\sqrt{K}$ measures the volume. To monitor scaling violations a different symbol is used for each value of $\beta = 6/g_0^2$, i.e. a . In

this format it is impossible to give proper credit to those who performed the simulations. For the same plot, but with symbols keyed by reference, see ref. [38]. The scaling violations are smaller than the (quoted) statistical uncertainties, so it is impossible to extrapolate in a . Not all error bars in fig. 7 are correct, mostly because not all original authors gave error bars for mass ratios. Therefore, uncertainties quoted in the original work have been added in quadrature, modified by reasonable assumptions for the correlations. Another source of error is that some of the original fits did not include correlations in the uncertainties of the data, and others did not do a fit at all. Finally, the uncertainties shown are statistical only. The purpose of the plot is to estimate lattice-spacing and finite-size effects. The curves at small $z\sqrt{K}$ are analytical; the agreement with Monte Carlo simulations is good, bolstering confidence in the numerical results. In a finite (cubic) box, the five $J = 2$ states split into a doublet E and a triplet T_2 . At large $z\sqrt{K}$ one sees a restoration of rotational symmetry, as these multiplets become degenerate, although there is not much data for T_2 . On the other hand, the statistical errors are still too large to discern scaling violations.

For several reasons the status of the spectrum of quark-model hadrons (π , ρ , p , Δ , ...) will not be discussed here. It is reviewed annually at conferences and the conclusion usually drawn is that it is not worth sharing with non-experts [40]. The two main problems are the quark mass and the quenched approximation. For small quark masses the algorithms for solving eq. (10.5) slow down immensely. On present computers one-year projects use quark masses near 400 MeV. The systematic errors introduced by the quenched approximation and the too-large quark masses are difficult to estimate accurately, and semi-quantitative methods suggest they are large. For example, to the extent that one believes chiral perturbation theory at $m_{u,d} = 400$ GeV, the proton mass is off by around 100% [41].

10.2 A Weak Matrix Element

This section gives an example of the long-term utility of lattice QCD. In electro-weak phenomenology unknown hadronic matrix elements often are the most significant theoretical uncertainty. Without reliable calculations of these matrix elements it is impossible to determine fundamental quantities, such as the Cabibbo-Kobayashi-Maskawa matrix, from experimental data. Since a recent summer-school article reviews the subject nicely [42], we will consider just one example.

In his lectures Yosef Nir stressed the importance of the ratio

$$B_K = \frac{3\langle \bar{K}^0 | \mathcal{O}_{\Delta S=2} | K^0 \rangle}{8m_K^2 f_K^2}, \quad (10.25)$$

and a related quantity $\hat{B}_K = B_K \alpha_s^{-2/9}$. The ingredients are the four-quark operator

$$\mathcal{O}_{\Delta S=2} = \bar{s}_a \gamma_\mu (1 - \gamma_5) d_a \bar{s}_b \gamma_\mu (1 - \gamma_5) d_b, \quad (10.26)$$

where a and b denote color indices, and the kaon decay constant f_K , given by a hadronic matrix element of an axial current

$$m_K f_K = \langle 0 | A_0^{\Delta S=1} | K^0 \rangle, \quad A_\mu^{\Delta S=1} = \bar{s} \gamma_\mu \gamma_5 d. \quad (10.27)$$

The mass enters eq. (10.27) when the K^0 is at rest.

The first step is to find a good kaon operator

$$\Phi_K = \int d^3x d^3y \bar{d}(\mathbf{x}) \gamma_5 s(\mathbf{y}) f(\mathbf{x}, \mathbf{y}), \quad (10.28)$$

such that

$$C_K(t) = \langle \Phi_K^\dagger(t) \Phi_K(0) \rangle = |\langle K^0 | \Phi_K | 0 \rangle|^2 e^{-m_K t} + \dots \quad (10.29)$$

has as little contamination from higher mass states (denoted by \dots) as possible. This is done during the mass-spectrum calculation, and yields m_K as a function of the gauge coupling and the quark masses, as well as $\langle K^0 | \Phi_K | 0 \rangle$.

Next compute f_K from the two-point correlator

$$C_2(t) = \langle A_0^{\Delta S=1}(t) \Phi_K(0) \rangle = \langle 0 | A_0^{\Delta S=1} | K^0 \rangle \langle K^0 | \Phi_K | 0 \rangle e^{-m_K t} + \dots \quad (10.30)$$

Here the choice of Φ_K is important: Since the current is a point-like operator, it does not couple well to the kaon. Hence, if $C_2(t)$ relies entirely on Φ_K to provide a good signal before the noise takes over.

Finally, compute a three-point correlator to get the numerator of eq. (10.25).

$$C_3(t_1, t_2) = \langle \Phi_K(t_1) \mathcal{O}_{\Delta S=2}(t_2) \Phi_K(0) \rangle. \quad (10.31)$$

For $t_1 > t_2$ (and t_2 and $t_1 - t_2$ large enough)

$$C_3(t_1, t_2) = \langle 0 | \Phi_K | \bar{K}^0 \rangle \langle \bar{K}^0 | \mathcal{O}_{\Delta S=2} | K^0 \rangle \langle K^0 | \Phi_K | 0 \rangle e^{-m_K t_1} \quad (10.32)$$

and a fit yields the numerator. Numerically nicer is to take a ratio:

$$\frac{C_3(t_1, t_2)}{C_K(t_1)} = \langle \bar{K}^0 | \mathcal{O}_{\Delta S=2} | K^0 \rangle \quad (10.33)$$

expecting a constant for suitable t_2 , or

$$\frac{C_3(t_1, t_2)}{C_2(t_1 - t) C_2(t)} = B_K, \quad (10.34)$$

again expecting a constant for suitable t_2 and t . In ratios such as these statistical errors cancel significantly because Monte Carlo fluctuations in numerator and denominator are strongly correlated.

By the way, for $t_2 > t_1$ (and t_1 and $t_2 - t_1$ large enough)

$$C_3(t_1, t_2) = \langle 0 | \mathcal{O}_{\Delta S=2} | K^0 K^0 \rangle \langle K^0 K^0 | \Phi_K | K^0 \rangle \langle K^0 | \Phi_K | 0 \rangle e^{-m_K(2t_2 - t_1)}; \quad (10.35)$$

for technical reasons the matrix element $\langle 0 | \mathcal{O}_{\Delta S=2} | K^0 K^0 \rangle$ will be needed below.

Exercise 10.4 To extract $\langle 0 | \mathcal{O}_{\Delta S=2} | K^0 K^0 \rangle$ one also needs $\langle K^0 K^0 | \Phi_K | K^0 \rangle$. Show how to get this from the four-point correlator $\langle \Phi_K^\dagger(t_1) \Phi_K^\dagger(t_1) \Phi_K(t_2) \Phi_K(0) \rangle$.

In summary, B_K and f_K are computed from three correlation functions, C_K , C_2 , and C_3 . However, depending on whether one uses Wilson or staggered fermions, there are a variety of difficulties. The details below may seem technical, but the underlying issue is the non-perturbative definition of composite operators.

First we shall discuss currents, needed for f_K . In both fermion formulations the chiral current algebra is broken by the lattice, cf. sect. 5. Hence, one must determine finite normalization constants for the currents. They can be calculated in perturbation theory, but it is also possible to compute them non-perturbatively [43]. For N_f Wilson fermions the correctly normalized vector (\bar{V}) and axial-vector (\bar{A}) currents are

$$\begin{aligned}\bar{V}_\mu^a &= \kappa_V V_\mu^a, \quad a = 0, \dots, N_f^2 - 1 \\ \bar{A}_\mu^a &= \kappa_A A_\mu^a, \quad a = 1, \dots, N_f^2 - 1 \\ \bar{A}_\mu^0 &= Z_A \kappa_A A_\mu^0,\end{aligned}\tag{10.36}$$

where the unbarred currents are expressed by products of canonically normalized quark fields. As in the continuum, the singlet axial current \bar{A}_μ^0 also has a $\ln(a)$ -dependent renormalization factor Z_A . The Wilson action preserves the vector symmetries, so, by Noether's theorem, there is a conserved vector current. The Ward identity for this current shows $\kappa_V = 1$. However, the Noether choice of V_μ is not always the most convenient in numerical calculations, and for other choices $\kappa_V \neq 1$. Similarly, all axial symmetries are broken, so $\kappa_A \neq 1$, for any choice of A_μ .

There are similar formulae for N_f staggered fermion fields [44]. Because of doubling, there are $4N_f$ fermion flavors staggering about. The κ factors depend on the flavor associated with doubling. In general, $\kappa \neq 1$, but the $U(N_f) \times U_\epsilon(N_f)$ chiral symmetry guarantees that, by Noether's theorem, there are N_f^2 conserved vector currents and N_f^2 (partially) conserved axial vector currents. Fortunately, a conserved axial vector current can be used to compute f_K .

The broken chiral symmetry of Wilson fermions leads to two serious problems in defining $\mathcal{O}_{\Delta S=2}$. The first problem is one of operator mixing. In a convenient jargon the operator $\mathcal{O}_{\Delta S=2}$ is called "LL," because it is superficially the product of two left-handed currents, cf. eq. (10.26). When the chiral symmetry is explicitly broken, it mixes with the associated "RR" and "LR" operators. ("R" implies the substitution $1 - \gamma_5 \rightarrow 1 + \gamma_5$.) The mixing can be computed in perturbation theory, and then the perturbatively corrected lattice approximant to the continuum operator can be used in eqs. (10.31). The second problem is the lack of chiral behavior of the matrix elements. Expanding in m_K^2

$$\langle \bar{K}^0 | \mathcal{O}_{\Delta S=2} | K^0 \rangle = \alpha + (\beta + \gamma) m_K^2\tag{10.37}$$

and

$$\langle 0 | \mathcal{O}_{\Delta S=2} | K^0 K^0 \rangle = \alpha + (\beta - \gamma) m_K^2.\tag{10.38}$$

Chiral symmetry would require that α and β vanish. But for Wilson fermions, with explicit breaking, the physically interesting quantity γ must be determined by subtracting these two matrix elements. Unfortunately, the difference has a larger statistical uncertainty than the individual terms.

For staggered fermions the continuous chiral symmetry implies $\alpha = \beta = 0$, but the remaining doubling poses problems. Moreover, to fully exploit the chiral symmetry both the pion and the kaon should be Goldstone bosons of the $U(1) \times U_\epsilon(1)$ symmetry [45]. Therefore, the calculations are performed with N_f valence quark fields and, hence, $4N_f$ flavors. Each quartet has a mass corresponding to a quark found in nature. (In a full QCD calculation, one would still use two or three dynamical quarks.) Roughly speaking,

it is straightforward to work out the correct tree-level normalization for $\mathcal{O}_{\Delta S=2}$, including factors of $3/4N_f$ to count flavors. Then the Ward identities of chiral symmetry take over, ensuring the normalization in the presence of interactions.

A generic problem is mixing with operators of lower dimension. Since the coefficients of these operators contain inverse powers of a there is no reliable method to remove them perturbatively. The only feasible way to remove these them non-perturbatively is to insist on the (continuum) chiral behavior. For the case at hand, these problems fortunately play no role, because $\mathcal{O}_{\Delta S=2}$ is the lowest dimension operator with $\Delta S = 2$.

There is no physical reason to prefer B_K to the matrix element $\langle \bar{K}^0 | \mathcal{O}_{\Delta S=2} | K^0 \rangle$. In addition to reduced statistical errors, the systematic errors associated with quenching are thought to be less for B_K than for $m_K f_K$ or $\langle \bar{K}^0 | \mathcal{O}_{\Delta S=2} | K^0 \rangle$ separately. The calculations with the smallest uncertainties have been done with staggered fermions [46]. At present the largest uncertainty comes from extrapolating in a ; it is uncertain whether the extrapolation should be taken in a or a^2 . The most recent results [47] are $\hat{B}_K = 0.66 \pm 0.06$ after a linear extrapolation and $\hat{B}_K = 0.79 \pm 0.03$ after a quadratic extrapolation. By comparison, Wilson quarks yield 0.88 ± 0.13 [48].

10.3 Renormalized Coupling Constant

The fundamental parameter in QCD is the renormalized coupling constant α_S . Traditionally it has been determined from high energy scattering experiments, using perturbative QCD as a tool. There are two drawbacks to this approach. First, the perturbative calculations are much harder than in QED, so it is unlikely that many multi-loop calculations will be done soon. Second, the processes most sensitive to α_S also involve hadronization of quarks, a non-perturbative effect that is difficult to calculate in a way both fundamental and reliable.

Another way to determine α_S is to use a low-energy quantity as experimental input and lattice gauge theory as the theoretical tool. The calculation hinges on a good choice of the fiducial parameter to set the scale. One a is known, the bare coupling $g_0^2(a)$ can be related to a more familiar coupling such as $g_{\overline{\text{MS}}}^2(\Lambda)$ via relations such as eq. (7.11). The spin-averaged splitting $\Delta m = m_{h_c} - \frac{1}{4}(3m_{J/\psi} + m_{\eta_c}) = 458.6 \pm 0.4$ MeV is an excellent choice for several reasons. The spin-averaging removes the sensitivity to the most important term in the improvement of Wilson fermions. (For quarks not nearly massless, there is no reason to use staggered fermions.) Potential models, which give a good empirical description of the ψ and Υ systems, show that there is a wide range of the quark mass, spanning charm and bottom, for which Δm is constant. Light quarks modify the results in two ways: at short distances they change the β function, and at long distances they lead to a breakdown in potential-model description. The former effect is discussed below. The latter is small below the open charm (or bottom) threshold.

For a lattice determination of α_S to compete with the traditional ones, the error analysis must be thorough. We shall see that statistical errors play almost no role once they are small enough to study the systematic effects. Table 1 contains the raw data of the simulations. Each ensemble (labeled by lattice size and β) consists of 25 configurations generated in the quenched approximation. The Monte Carlo calculation

Table 1: Raw data for $\alpha_{\overline{\text{MS}}}$ calculation. The errors are statistical only.

lattice	β	$a\Delta m$	a^{-1} (GeV)	$\langle \text{Tr } U_P \rangle$	$\alpha_{\overline{\text{MS}}}^{(0)}(5 \text{ GeV})$
$12^3 \times 24$	5.7	0.399(26)	1.15(8)	0.549	0.1333(23)
16^4	5.9	0.258(13)	1.78(9)	0.582	0.1371(46)
24^4	6.1	0.189(12)	2.43(15)	0.605	0.1382(56)

provides $a\Delta m$, which defines a . The $\overline{\text{MS}}$ coupling is obtained from eq. (7.11)

$$\frac{1}{g_{\overline{\text{MS}}}^2(\pi/a)} = \frac{1}{g_0^2} \langle \text{Tr } U_P \rangle + 0.025 \quad (10.39)$$

using $N = 3$ and $N_f = 0$, where $\langle \text{Tr } U_P \rangle = 1 - \langle P_{\mu\nu} \rangle$. Instead of the perturbative value $\langle P_{\mu\nu} \rangle = \frac{1}{3}g_0^2$, the non-perturbative value in the fifth column of Table 1 was used. This accounts for higher-order corrections to eq. (7.11). In the sixth column of Table 1 the two-loop renormalization group equation was used to convert π/a to a standard scale 5 GeV. The superscript on $\alpha_{\overline{\text{MS}}}$ denotes the number of flavors: $N_f = 0$ because the ensembles were generated without fermions.

The results in the sixth column of Table 1 have a small but noticeable scaling violation. Extrapolating in a^2 leads to $\alpha_{\overline{\text{MS}}}^{(0)}(5 \text{ GeV}) = 0.1431 \pm 0.0028$. One might expect $\mathcal{O}(g_0 a)$ corrections to be present because the quarks have been treated using the improved Wilson action. However, one of Δm 's appealing traits is that $\bar{\psi}\sigma_{\mu\nu}C_{\mu\nu}\psi$ does not affect it. Hence, the scaling violations are more likely proportional to a^2 . The data favor it too.

The last step is to correct for the quenched approximation. The original justification for the quenched approximation can be re-phrased by treating it as an effective field theory for full QCD. In other words, one would like to know what value of $\alpha_{\overline{\text{MS}}}^{(N_f)}(5 \text{ GeV})$ produces the same charmonium physics as a given value of $\alpha_{\overline{\text{MS}}}^{(0)}(5 \text{ GeV})$. The shift is

$$\frac{1}{g_{N_f}^2(\pi/a)} - \frac{1}{g_0^2} = 2 \int_{\mu}^{5 \text{ GeV}} d \ln q \left[\beta_0^{(N_f)} - \beta_0^{(0)} + (\beta_1^{(N_f)} - \beta_1^{(0)})g^2 \right], \quad (10.40)$$

where the subscript on g now denotes N_f and the β function coefficients are given in eq. (7.5). Rather than $g_{\overline{\text{MS}}}$ it makes more sense to use a physical definition of the coupling, such as the one defined by the heavy-quark potential. Choosing a range of μ suited to momentum scales present in charmonium leads to a correction and an uncertainty. The final result [49] is

$$\alpha_{\overline{\text{MS}}}^{(4)}(5 \text{ GeV}) = 0.174 \pm 0.012, \quad (10.41)$$

or, for comparison to LEP experiments,

$$\alpha_{\overline{\text{MS}}}^{(4)}(M_{Z^0}) = 0.105 \pm 0.004. \quad (10.42)$$

The dominant source of uncertainty stems from integrating eq. (10.40), because μ must be chosen so low that the perturbative β function is no longer reliable. Monte Carlo calculations on the next generation of computers will not use the quenched approximation (for this calculation) so this uncertainty will vanish. Nevertheless, despite the quenched approximation lattice gauge theory is already competitive with traditional determinations of α_s .

Similar calculations have been performed for both ψ and Υ [51] using a non-relativistic formulation of lattice fermions [50]. The results are compatible with eq. (10.41). This is significant for two reasons. First, the general pattern of lattice-spacing errors are different for Wilson and non-relativistic fermions. Hence, agreement between the two charmonium calculations shows that the lattice-spacing extrapolations are under control. Furthermore, the Υ system is much less sensitive to ambiguities in μ , which is roughly three times larger than for ψ .

There is an uncertainty that is not quoted in eq. (10.41). At several stages of the analysis perturbation theory was used, in particular in eqs. (10.39) and (10.40). For comparison with traditional determinations that is fair, because they are explicitly based on perturbation theory, and hence contain the same uncertainty, also not quoted. Obviously, it is desirable to eliminate this uncertainty and compute everything from first principles non-perturbatively. An especially clever technique exploits the finite physical volume of lattice calculations [52]. The resulting coupling will be the new standard for α_s , because it will have negligible uncertainty. It is important that the new standard will be a physical quantity that can also be calculated in perturbation theory. Then formulae analogous to eq. (7.11) can be used to convert existing expansions to the new standard. In summary, QCD (non-perturbative plus perturbative) will predict high-energy scattering cross sections using $\Delta m = 458.6$ MeV as input. Unless QCD is wrong, we will find agreement.

Acknowledgements

First, I thank the students of TASI '91. Without them there would have been no reason to give the lectures. I would like to thank Keith Ellis, Chris Hill, and Joe Lykken for inviting me. Their splendid organization, together with K.T. Mahanthappa and everyone else at the University of Colorado, made everything run smoothly. Finally, I am grateful to Aida El Khadra and Tao Han for their help in preparing the written version.

References

- [1] K.G. Wilson and J. Kogut, *Phys. Reports* **12C** (1974) 75.
- [2] M. Creutz, *Phys. Rev.* **D15** (1977) 1128.
- [3] M. Lüscher, *Commun. Math. Phys.* **54** (1977) 283.
- [4] F. Wegner, *Phys. Rev.* **B5** (1972) 4529.
- [5] K.G. Wilson, in *New Phenomena in Subnuclear Physics*, edited by A. Zichichi (Plenum, New York, 1977).

- [6] H.B. Nielsen and H. Ninomiya, *Nucl. Phys.* **B185** (1981) 20, (E) **B195** (1982) 541; *ibid.* **B193** (1981) 173.
- [7] L. Susskind, *Phys. Rev.* **D16** (1977) 3031.
T. Banks, J.B. Kogut, and L. Susskind, *Phys. Rev.* **D13** (1976) 1043.
- [8] N. Kawamoto and J. Smit, *Nucl. Phys.* **B192** (1981) 100.
- [9] H.S. Sharatchandra, H.J. Thun and P. Weisz, *Nucl. Phys.* **B192** (1981) 205.
- [10] H. Leutwyler, this volume
- [11] K.G. Wilson, *Phys. Rev.* **D10** (1974) 2445.
- [12] H. Kawai, R. Nakayama, and K. Seo, *Nucl. Phys.* **B189** (1981) 40.
- [13] M. Lüscher and P. Weisz, *Nucl. Phys.* **B266** (1986) 309.
- [14] T. Reisz, *Commun. Math. Phys.* **116** (1988) 81, 573, *ibid.* **117** (1988) 79, 639.
- [15] G. Sterman, this volume
- [16] P. Weisz, *Phys. Lett.* **100B** (1981) 331. A. Hasenfratz and P. Hasenfratz, *Phys. Lett.* **93B** (1980) 165.
- [17] G.P. Lepage and P.B. Mackenzie, FERMILAB-PUB-91/355-T.
- [18] R. Dashen and D. Gross, *Phys. Rev.* **D23** (1981) 2340.
- [19] A.S. Kronfeld and D.M. Photiadis, *Phys. Rev.* **D31** (1985) 2939.
- [20] Early references include K. Wilson, in *Recent Developments in Gauge Theories*, edited by G. 't Hooft et al (Plenum, New York, 1980).
K. Symanzik, in *Mathematical Problems in Theoretical Physics*, edited by R. Schrader et al (Springer, Berlin, 1982); *Nucl. Phys.* **B226** (1983) 187, 205.
P. Weisz, *Nucl. Phys.* **B212** (1983) 1.
G. Curci, P. Menotti, and G. Paffuti, *Phys. Lett.* **130B** (1983) 205.
P. Weisz and R. Wohlert, *Nucl. Phys.* **B236** (1984) 397.
- [21] M. Lüscher and P. Weisz, *Commun. Math. Phys.* **97** (1985) 59; (E) **98** (1985) 433.
- [22] B. Sheikholeslami and R. Wohlert, *Nucl. Phys.* **B259** (1985) 572.
- [23] A.X. El Khadra, FERMILAB-CONF-92/10-T.
- [24] G. Heatlie, C.T. Sachrajda, G. Martinelli, C. Pittori, and G.C. Rossi, *Nucl. Phys.* **B352** (1991) 266.
- [25] M. Lüscher and P. Weisz, *Nucl. Phys.* **B240** (1984) 349.
- [26] For a review of various approaches see P. Hasenfratz, *Nucl. Phys. B(Proc. Suppl.)* **9** (1989) 3.
- [27] J. Kuti, L. Lin, and Y. Shen, *Phys. Rev. Lett.* **61** (1988) 678.

- [28] M. Lüscher and P. Weisz, *Nucl. Phys.* **B290** (1987) 25; *ibid.* **B295** (1988) 65.
- [29] G.A. Baker and J.M. Kincaid, *J. Stat. Phys.* **24** (1981) 469.
- [30] M. Lüscher and P. Weisz, *Phys. Lett.* **B212** (1988) 472; *Nucl. Phys.* **B318** (1989) 705;
- [31] K.G. Wilson, ref. [20].
- [32] D.H. Weingarten and D.N. Petcher, *Phys. Lett.* **99B** (1981) 333.
G.G. Batrouni, G.R. Katz, A.S. Kronfeld, G.P. Lepage, B. Svetitsky, and K.G. Wilson, *Phys. Rev.* **D32** (1985) 2736.
- [33] S. Duane, A.D. Kennedy, B. Pendleton, and D. Roweth, *Phys. Lett.* **B195** (1987) 216.
- [34] D. Weingarten, *Phys. Lett.* **109B** (1982) 57.
- [35] A. Morel, SACLAY-PhT/87-020.
S.R. Sharpe, *Phys. Rev.* **D41** (1990) 3233.
- [36] C. Bernard and M. Golterman, to appear in *Nucl. Phys. B(Proc. Suppl.)*.
- [37] F. Brandstaeter, A.S. Kronfeld, and G. Schierholz, *Nucl. Phys.* **B345** (1990) 709
- [38] A.S. Kronfeld, in *Intersections between Nuclear and Particle Physics*, edited by W.T.H van Oers (AIP, New York, 1992).
- [39] C.T.H. Davies, G.G. Batrouni, G.R. Katz, A.S. Kronfeld, G.P. Lepage, K.G. Wilson, P. Rossi, and B. Svetitsky, *Phys. Rev.* **D37** (1988) 1581.
- [40] T. DeGrand, *Nucl. Phys. B(Proc. Suppl.)* **20** (1991) 353.
D. Toussaint, to appear in *Nucl. Phys. B(Proc. Suppl.)*.
- [41] J. Gasser and H. Leutwyler, *Phys. Reports* **87** (1982) 77.
- [42] C. Bernard, in *From Actions to Answers*, edited by T. DeGrand and D. Toussaint (World Scientific, Singapore, 1990).
- [43] M. Bochicchio, L. Maiani, G. Martinelli, G.C. Rossi and M. Testa, *Nucl. Phys.* **B262** (1985) 331.
L. Maiani, G. Martinelli, G.C. Rossi and M. Testa, *Nucl. Phys.* **B289** (1987) 505.
- [44] M.F.L. Golterman and J. Smit, *Nucl. Phys.* **B245** (1984) 61. J. Smit and J. Vink, *Nucl. Phys.* **B298** (1988) 557.
- [45] G.W. Kilcup and S.R. Sharpe, *Nucl. Phys.* **B283** (1987) 493.
- [46] G.W. Kilcup, S.R. Sharpe, R. Gupta, and A. Patel, *Phys. Rev. Lett.* **64** (1990) 25.
- [47] S.R. Sharpe, CEBAF-TH-92-01.

- [48] C. Bernard, T. Draper, G. Hockney, and A. Soni *Phys. Rev. D* **38** (1988) 3540.
M.B. Gavela, L. Maiani, S. Petrarca, F. Rapuano, G. Martinelli, O. Pene, and C.T. Sachrajda, *Nucl. Phys. B* **306** (1988) 677.
- [49] A.X. El Khadra, G.M. Hockney, A.S. Kronfeld, and P.B. Mackenzie, FERMILAB-PUB-91/354-T.
- [50] G.P. Lepage and B.A. Thacker, *Nucl. Phys. B(Proc. Suppl.)* **4** (1988) 199.
- [51] C.T.H. Davies, G.P. Lepage, and B.A. Thacker, to appear in *Nucl. Phys. B(Proc. Suppl.)* and elsewhere.
- [52] M. Lüscher, P. Weisz, and U. Wolff, *Nucl. Phys. B* **359** (1991) 221.